CHALMERS
UNIVERSITY OF TECHNOLOGY

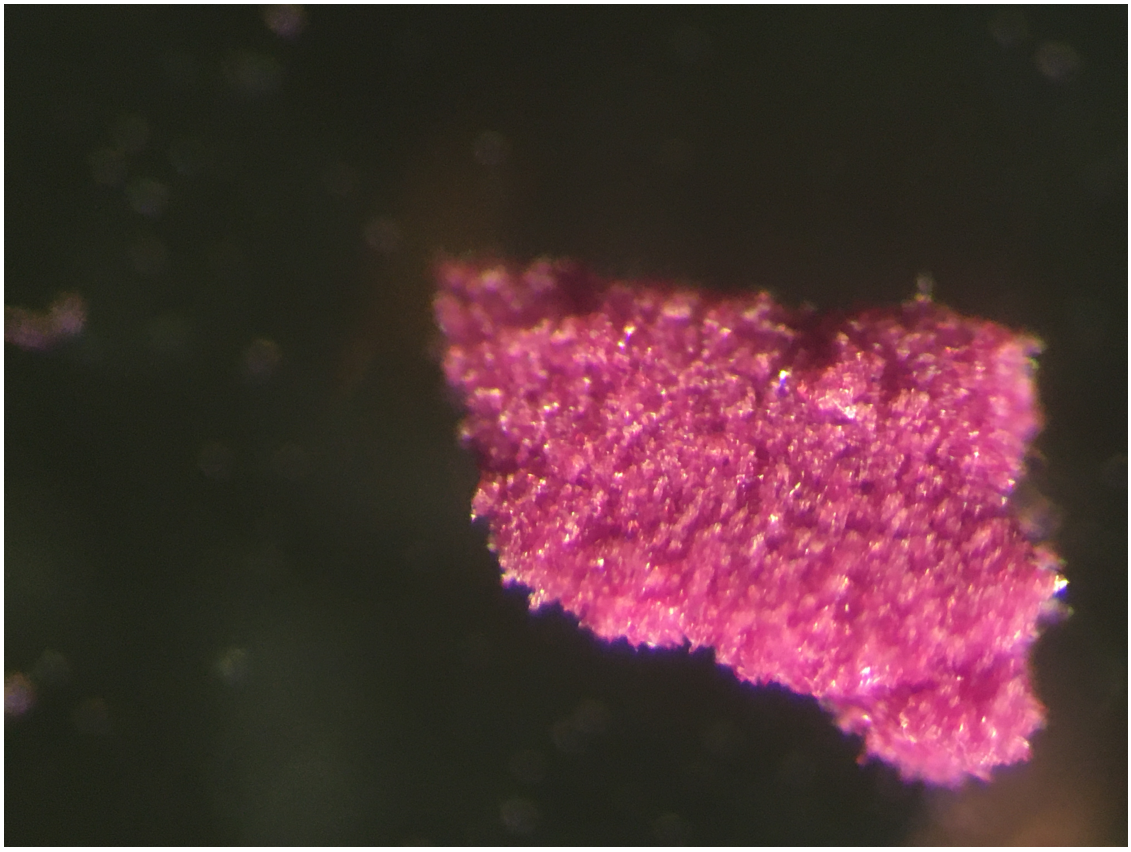

Synthesis and development of metal-organic frameworks with focus on hexagon 3D topologies

Master's thesis in Materials Chemistry

Victor Engdahl

Department of Chemistry and Chemical Engineering
CHALMERS UNIVERSITY OF TECHNOLOGY
Gothenburg, Sweden 2020

Master's thesis 2020

Synthesis and development of metal-organic frameworks with focus on hexagon 3D topologies

Synthesizing old and new MOF topologies in order to gather information about MOF structures to further develop the knowledge in synthesis of structures and their attained properties

VICTOR ENGDAHL

CHALMERS
UNIVERSITY OF TECHNOLOGY

Department of Chemistry and Chemical Engineering
Chalmers University of Technology
Gothenburg, Sweden 2020

Synthesis and development of metal-organic frameworks with focus on hexagon 3D topologies
Synthesizing old and new MOF topologies in order to gather information about MOF structures to further develop the knowledge in structure synthesis and its attained properties
VICTOR ENGDAHL

Supervisor: Lars Öhrström, Division of Chemistry and Biochemistry
Examiner: Jerker Mårtensson, Division of Chemistry and Biochemistry

Master's Thesis 2020
Department of Chemistry and Chemical Engineering
Chalmers University of Technology
SE-412 96 Gothenburg
Telephone +46 73 092 7013

Cover: Visualization of synthesized cobalt complex viewed in a microscope, specifically sample VE-Co1.

Gothenburg, Sweden 2020

Synthesis and development of metal-organic frameworks with focus on hexagon 3D topologies

VICTOR ENGDAHL
Department of Chemistry and Chemical Engineering
Chalmers University of Technology

Abstract

The focal point of the thesis was on the synthesis of Metal-Organic Frameworks (MOFs) and especially MOFs with hexagon-based topologies. MOFs are single-and multi- dimensional materials made of metal ions and organic ligands held together by coordination bonds and having potential porosity. Hexagon-based topologies of MOFs are sought after due to their scarcity in the literature.

MOFs are tunable and flexible in structure as well as properties. This make them a promising material for making improvements in areas like catalysis and separation. To understand MOFs and how to tune them and achieve predetermined properties reticular chemistry is an essential tool.

Synthesis of MOFs was done through solvothermal synthesis. 23 samples of MOFs were made and analysed with Powder X-Ray Diffraction (PXRD), Thermogravimetric Analysis (TGA), Infrared spectroscopy (IR) and UV-light when appropriate.

The organic linker used was 1',2',3',4',5',6'-hexakis(4-carboxyphenyl)benzene (H_6cpb), and the metals in an ionic state was terbium, aluminum, zinc, cobalt, vanadium, manganese, zirconium, gadolinium and copper.

TGA, IR, and PXRD showed typical results for MOFs indicating that MOFs could have been formed. The main tool to estimate if a MOF had been synthesized was PXRD analysis. In the PXRD diffractograms two peaks at around 2 7° and 11° together with the lack of a peak at 16°, occurring for all solid forms known of the organic linker were taken as an indication of MOF formation.

Another important tool were the simulate XRD powder patterns of previously known MOF structures.

It is likely that at least one MOF, tentatively formulated as $[Tb_4(cpb)(acetato)_2(dmf)_4X4]$, was prepared as UV light showed the characteristic luminescence of terbium, the PXRD was different from the linker on its own, and IR and TGA data were compatible with MOF formation.

Due to Single Crystal X-Ray Diffraction (SCXRD) not being available at Chalmers, firm confirmation that other MOFs had been synthesized could not be obtained.

For future work, further structure analysis needs to be done on the possible MOFs.

Keywords: MOFs, hexagon, topology, reticular chemistry, solvothermal synthesis, PXRD, lanthanoids

Acknowledgements

I would like to thank my supervisor Lars Öhrström for providing the initial project direction and for making this project possible. Since I began with this master thesis he has been there to aid me with questions, new directions in the thesis, analysis and insightful discussions. This has continued well during the COVID-19 pandemic by answering e-mails quickly and in general to be available even during these times.

I would also like to thank Francoise Mystere Amombo Noa for the aid and expertise when it comes to synthesizing my samples as she provided previous knowledge and experience from the laboratory work she had done previously. She has also always been available over e-mail during this pandemic which is much appreciated.

I have also been given aid when Lars and Francoise have been out of town by Jerker Mårtensson, my examiner, and Michal Strach, scientist at Chalmers Materials Analysis Laboratory. Both have been of great importance when it came to questions regarding the chemistry involved and analysis of samples.

Finally, I would like to thank Axel Jonsson who had a similar thesis project as myself. He has been there since the beginning as someone I can always ask questions and have a discussion with about my work and his work and what we both could do to improve them. I also want to thank him for aiding me in running analysis of samples the last couple of weeks as I became ill and could not perform the last samples on my own in order finish the thesis work.

Victor Engdahl, Gothenburg, June 2020

Contents

List of Figures

List of Tables

List of Abbreviations

AcOH Acetic acid.
ATR Attenuated Total Reflectance.

COFs Covalent-Organic Frameworks.

DCM dichloromethane.
DMF N,N-Dimethylformamide.

FA Formic acid.

H_6cpb 1',2',3',4',5',6'-hexakis(4-carboxyphenyl)benzene.

IR Infrared spectroscopy.
IR Infrared spectroscopy.

LMET Ligand-to-Metal Energy Transfer.

MOFs Metal-Organic Frameworks.

ppb 4,4'-(3',4',5',6'-tetrakis(4-(pyridin-4-yl)phenyl)-[1,1':2',1"-terphenyl]-4,4"-diyl)dipyridine.
PXRD Powder X-Ray Diffraction.

SAXS Small Angle X-ray Scattering.
SBUs Secondary Building Units.
SCXRD Single Crystal X-Ray Diffraction.
SEM Scanning-Electron Microscopy.

TEM Transmission Electron Microscopy.
TGA Thermogravimetric Analysis.

WAXS Wide Angle X-ray Scattering.

1
Introduction

The main focus of this master thesis is the synthesis of Metal-Organic Frameworks, MOFs, to further increase the amount of known MOF structures. This will aid in finding and utilizing the new properties that can be achieved with these materials and in the end find applications which could improve human living standards.

MOFs are single- and multi-dimensional materials consisting of primarily metal ions and organic ligands which are held together by coordination bonds[1]. According to the International Union of Pure and Applied Chemistry (IUPAC) recommendations of MOF terminology from 2013, the definition of a MOF is "a coordination network with organic ligands containing potential voids"[2].

Reticular chemistry is a major part of this thesis especially when it comes to exploring the possibility of creating MOFs which has 3D hexagon-based topologies. Reticular chemistry is generally described as the chemistry that uses molecules together with bonds of different strengths to create open crystalline frameworks[3]. Finding MOFs with 3D hexagon-based topologies is important since there is a lack of such topologies in the literature. The main goal is to synthesize new MOF structures especially MOFs with hexagon 3D topolgies.

The hypothesis of this thesis is that using H_6cpb with especially the larger metal ions from the lanthanoids series, a MOF with a hexagon-based topology, can be created.

MOFs will have a part to play in the coming years when it comes to chemical applications. Synthesizing MOFs with new structures will assist in further enhancing the ability to design specific materials with predictable properties. But to do this a greater understanding is needed regarding how topologies and structures work and what they demand individually from the starting materials and synthesis conditions to form[3]. Which is the subject of reticular chemistry.

With the energy demand increasing in all parts of the world, there is also an increasing amount of fossil fuel used to satisfy this demand. This leads to higher emissions and a more brute forced energy production. To solve this, there are different solutions. Some areas in which MOFs can assist are in the areas of solar panel efficiency, nuclear waste management, gas adsorption and catalysis. This could be done through functionalization of MOFs to target certain applications, which is the core function of using reticular chemistry for application development.

1.1 Aim of the project

The aim is to synthesize MOFs with the larger and more scarcely used metal ions in the periodic table to hopefully synthesize a new MOF with 3D hexagon-based topology. After the synthesis, the structure will be determined. If there is time, certain properties like CO_2 adsorption and I_2 adsorption will be investigated for the synthesized MOFs. Other topologies and structures that are new, which are not for example 3D hexagon topologies, will still be investigated.

1.2 Method

In this section the work process will be discussed as well as introduction to what type of analysis will be performed. The work process can be viewed in Figure 1.1.

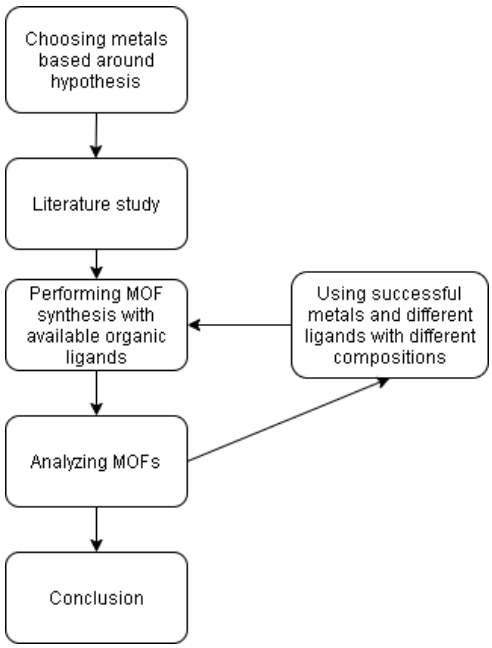

Figure 1.1: Scheme of how the work process will look during thesis work.

Analysis of MOFs was performed using a series of analyzing methods which are PXRD, TGA and elemental analysis. Using these methods, the structures of the synthesized MOFs was investigated and the potential applications of the MOFs were evaluated by reviewing their properties

1.3 Limitations

This project work will not cover the synthesis of the organic ligands used as they will be provided by Mr. Steffen Brülls. The project will focus on small scale synthesis of MOFs through solvothermal synthesis.

If a specific synthesized MOF has some promising properties towards a certain application, refinement of this MOF by changing its composition to further improve the MOFs

application possibilities will be performed. This may reduce the total amount of attempts with other metal and ligand combinations.

Not all analytical procedures will be performed during this thesis as the samples synthesized will be sent for analysis to different researchers and different locations. The procedures, if possible, will be experienced in the thesis at least once and thereafter as much as there is time for. SCXRD was supposed to be the main analysis tool, but PXRD was used instead. Other possible experiments will be performed if a crystalline MOF is found.

As the project progresses, certain MOFs with certain properties will be focused on. For example, if a created MOF is suitable for CO_2 adsorption/conversion the project might turn towards those specific applications and those MOFs as they show promising results.

Due to COVID-19 analysis of the different samples has been difficult and equipment like SCXRD and CO_2 adsorption have not been available. Therefore the use of PXRD has been the primary analysis method in this thesis as the pandemic escalated.

2
Theory

This chapter intends to provide more in-depth knowledge complementing the introduction section. The theory provided will also help advocate for the directions taken in the laboratory and to draw conclusions.

2.1 Reticular chemistry

Reticular chemistry is a practice that is utilized to bind the old ways with the new ways of specific property synthesis. Knowing the properties of the atoms and molecules binding it together with knowing the structure that also gives certain properties. Utilizing reticular chemistry enables micro-managing the structure in size, topologies, and properties which could be beneficial. The final goal would be to understand structures and bonds at such a level, that new molecules with a predetermined property can be created. The main examples of how this practice is used are within the molecule-based materials such as MOFs and COFs[3]. The reticular chemistry has therefore been accepted as "the chemistry of linking molecular building blocks by strong bonds into crystalline extended structures, such as Metal-Organic Frameworks (MOFs) and Covalent-Organic Frameworks (COFs)"[4]. Three main points can be used to better understand reticular chemistry, Yaghi concludes them as[3]

> (i) Molecular building blocks provide control in the construction of frameworks because of their well-defined structure and geometry, (ii) strong bonds impart architectural, thermal, and chemical stability to the resulting frameworks, and (iii) crystallinity, which was the challenge impeding the progress toward realizing such frameworks, ensures that their structures can be definitively characterized by X-ray or electron diffraction techniques.

From these three points, reticular chemistry aims to describe how building blocks build up structures, how these structures are stable through strong bonds between the nodes and that crystallinity is of importance for the analysis to be performed so that the relationship between structure and properties can be apprehended.

One way to explain how reticular chemistry can impact material formation, specifically for MOFs, is the ability to create the structure with certain properties. Since the building blocks are the same in the entire framework, a specific structural design in one part of the material gives the sought after property throughout the entire framework. This could for example be utilized in catalysis where there would be active sites in the entire molecule. MOFs can also work as a good separation tool for strongly bonded molecules as its structure can be controlled through reticular chemistry. This allows for separation of molecules like propylene from ethylene which is shown in the study by Dai and Sun et al.[5] where a MOF could perform this separation.

For the future of reticular chemistry to prosper the application-driven science, which can sometimes be prominent in today's research, has to be minimized. The structure of new frameworks is still valuable information to further increase the knowledge of reticular chemistry even without an application. This would increase the overall "reticular chemistry database" which would aid in actually finding applications[4].

The future of reticular chemistry lies in trying to increase the range at which topologies can be controlled. The goal is to go to a higher order like 2D or 3D instead of at only one point (0D) and a certain path (1D).

2.2 Metal-Organic Frameworks

MOFs are primarily made up of metal ions and organic ligands which are held together by coordinated bonds. This is the cornerstone of how MOFs get their structural properties. A MOF can have different structures with different building units but in general, they are still a crystalline solid with porous properties[6]. Other typical properties of MOFs are large surface area, tunable pore size, tunable surface chemistry, and multiple topologies. All these properties and that they can be tuned leads to MOFs being a versatile material[7].

In MOFs, the metal or metal clusters bind to the organic ligands. This cluster is then called a node. These nodes are essential for creating different geometries possible in MOFs. The vast amount of geometries that can be formed are called Secondary Building Units (SBUs)[1].

SBUs can be rigid so that the metal-part is stationary in a certain position with strong carboxylate bonds. This means the SBU goes from having one metal ion as its vertex to having the entire SBU as its vertex in a larger extended framework. These vertices together with the organic ligands have the potential to form a high framework stability[8].

The MOFs properties can be altered by changing the ligands, for example, carboxylate group ligands, which most MOFs are built with, can provide the MOFs with a more robust and rigid structure. This can be compared to if the ligand is then changed to a nitrogen ligand, in which case, the robustness of the structure lowers[1]. To usage of organic linkers to create rare 3D MOFs are typical for MOFs due to their tunable length and coordination chemistry[9].

Another function in MOFs is its ability to change properties by adding guest molecules. This procedure is a more recent way of changing properties. Adding guest molecules is possible due to the tunability of properties in MOFs, like the chemical environment inside the structure. This modification could make MOFs suitable for adsorption of new molecules, the so-called guest molecules[10]. These guest molecules could work to improve or find new applications in areas like hydrogen storage[11], chemical sensing[12], catalysis[13], and separation[14]. What is very convenient about these property changes is that the introduction of a guest molecule changes the properties without disturbing structural integrity. The main reason for MOFs being able to have good collaboration with a guest molecule is the fact that MOFs are crystalline and have strong coordinated bonds. The

crystalline structure of the MOFs makes them tuneable to a great extent compared to amorphous materials. The strong coordinated bonds can sometimes be extended beyond what is the metal cluster and the organic ligands and then involve these guest molecules. MOFs can also, if there are unsaturated sites, be suitable for interaction with guest molecules[10].

The main drawback of some MOFs is that they are unstable due to the natural reversibility of the coordination bonds compared to covalent bonds. To improve stability, post-treatments and post-modifications have been evaluated and proven effective. To further reduce this problem in MOFs there is larger research focus on trying to create inherently more stable MOFs[15]. The stability of the MOFs has been summarized to depend on a few parameters where some of the important ones are the pK_a of ligands[16], the oxidation state[17], the ionic radius of metal ions and their reduction potential[18], the coordination geometry and the hydrophobicity of the pore surface[19]. An example of a successfully stable MOF is the zirconium-based MOF called UiO-66 which was synthesized at Oslo University by Cavka et al[20].

One group of MOFs, called hexatopic hexagon-based topologies, is of interest to this thesis due to its scarcity in research. The hexatopic hexagon-based topologies have been investigated to some degree but still far less than some of the more basic structures[21]. These new hexagon structures are interesting since they could have new interesting properties and applications not seen before.

2.3 Specific topologies

Different kinds of 3D hexagon-based topologies are sought after in this thesis and the reason for this is the previous work made by Francoise Noa et al. In their work they figured that the **kgd**-net could become a 3D net by introducing larger ions in the voids present in the **kgd**-net. By changing the **kgd**-net to a 3D net a new 3D structure could perhaps be achieved called the **laf**-net. The **laf**-net is a foldable 3D net and it is the best-case scenario for the thesis, synthesizing a MOF with the **laf**-net topology.[22].

The more basic net, **kgd**, is a net that after it is formed results in 2D layers with trigonal and hexagonal SBUs. This means that in general, a metal salt is wanted that has a 3+ charge for the trigonal linking sites to take place. However, this can depend on your organic linker, which sits in the hexagonal linking space. If the organic linker in the hexagonal space is in a protonated state it can allow for bonding to a metal salt with a lower charge to 2+[23]. A visual representation of the **kgd**-net is presented in Figure 2.1

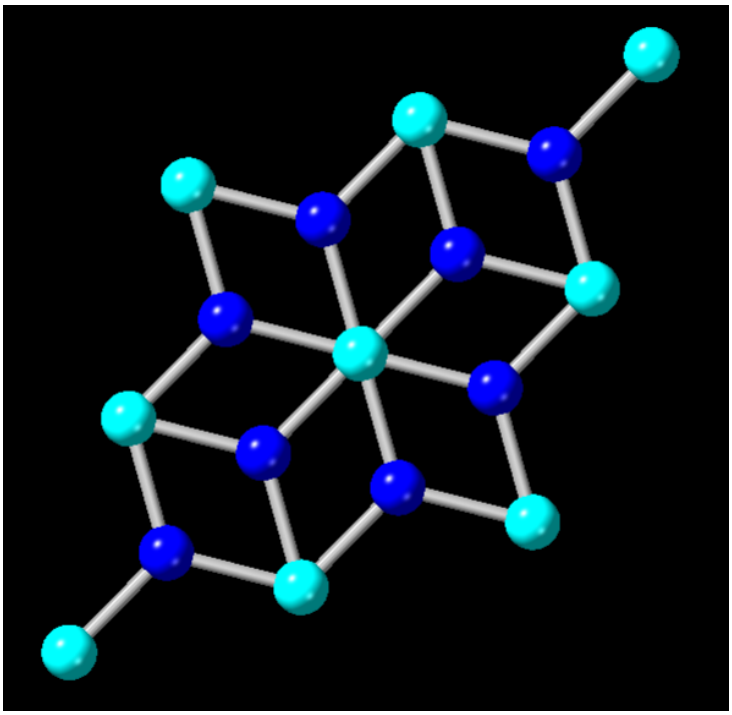

Figure 2.1: 2D representation of the 2D **kgd**-net

The new 3D structure, called the **laf**-net, is a foldable 3D structure with perfectly planar equilateral triangles and planar hexagons. The structure is foldable in the sense that it can fold on the tetragonal axis while still having stable hexagonal and triagonal SBUs. The structure of the **laf**-net can be seen in Figure 2.2.

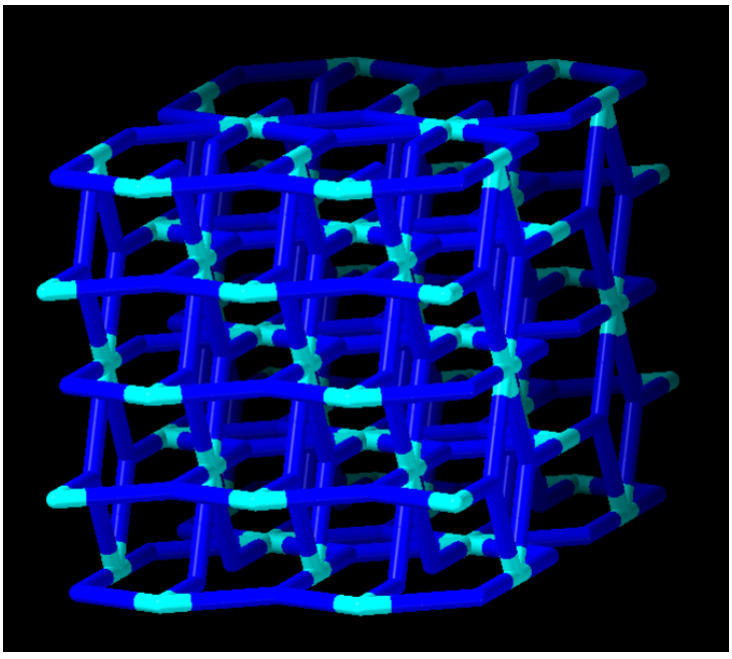

Figure 2.2: 3D representation of the **laf**-net

The main net sought after in this thesis is the **laf**-net but other nets are still of interest, like the **yav**-net. The **yav**-net is a net that has proven to form with some of the MOFs created with the linkers in this thesis in work done by Francoise Noa et al[22]. It is very similar to the **kgd**-net but instead of 2D its in 3D with the trigonal SBUs being trigonal

bi-pyramids. This means there are bonds between the layers, 5 bonds in total between every metal ion. This structure can be seen in Figure 2.3.

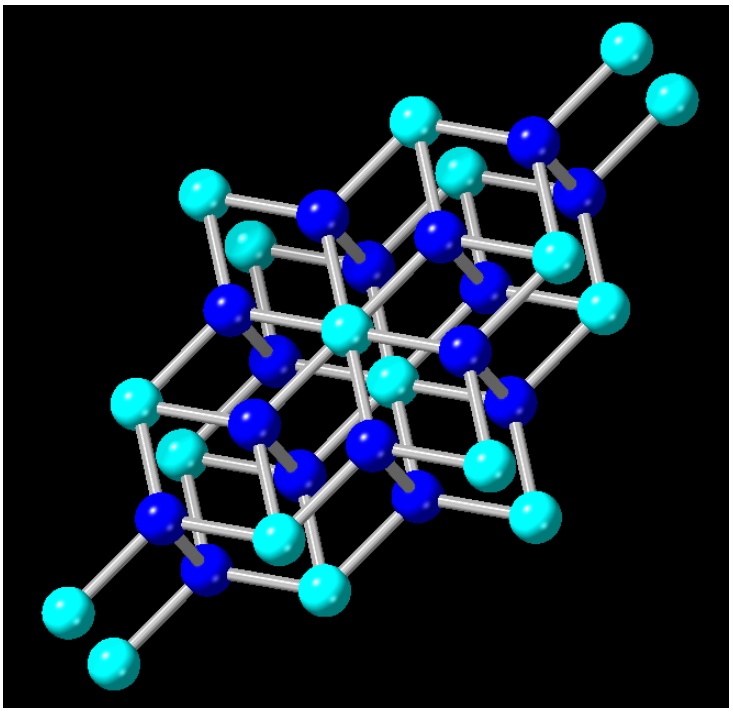

Figure 2.3: 3D representation of the **yav**-net

2.4 Organic linkers

In the thesis different linkers will be used as building blocks with the goal of synthesizing 3D hexagon-based MOFs. These linkers will work as the hexagonal linking point in the 3D nets described in the specific topologies section. The two organic linkers that will be used is H_6cpb and 4,4'-(3',4',5',6'-tetrakis(4-(pyridin-4-yl)phenyl)-[1,1':2',1"-terphenyl]-4,4"-diyl)dipyridine (ppb). These organic linkers can be seen in Figure 2.4.

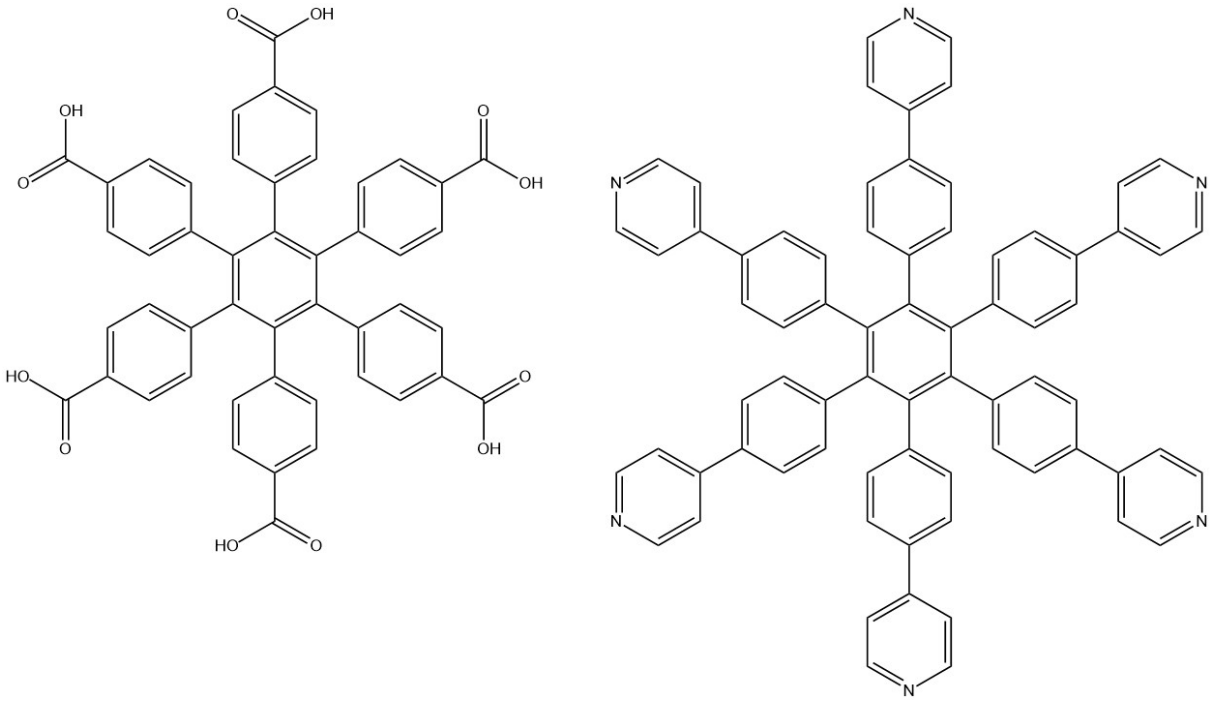

Figure 2.4: Structure drawing of the organic linkers. The organic linker H_6cpb to the left. The organic linker ppb to the right

2.5 Metal ions

The targeted metal ions that will be investigated are Tb^{3+}($TbCl_3{\cdot}6H_2O$), Al^{3+}($AlCl_3 \cdot 6H_2O$), Zn^{2+}($Zn(NO_3)_2 \cdot 6H_2O$ and $ZnCl_2$), Co^{2+}($Co(NO_3)_2 \cdot 6H_2O$), V^{3+}(VCl_3), Mn^{2+}($MnCl_2 \cdot 4H_2O$), Zr^{4+}($ZrOCl_2 \cdot 8H_2O$), Gd^{3+}($Gd(NO_3)_3 \cdot 6H_2O$) and Cu^{2+}($Cu(NO_3)_2 \cdot 6H_2O$).

Transition metals are the most common kind of metals to be used in the synthesis of MOFs together with metal ions like zinc. This is mainly due to the accessibility of different metal ions with different valance states and the different properties these metal ions have. These differences lead to very different MOF properties[24]. The largest drawback of these elements is that the usual synthesis route is solvothermal synthesis which requires high temperatures, sometimes additives like acids and long synthesis times[25].

Lanthanoids are a group of metals in the periodic table with larger ions. Within the f-block, the lanthanoids can be a part of a larger coordination sphere which makes them interesting in building MOFs that have larger SBUs. Lanthanoids with suitable organic linkers can achieve desirable properties within luminescence, magnetism, and catalysis[26].

The luminescence property is of interest to many due to the luminescence of the MOFs not being ordinary Stokes shifts, long lifetime, visible color, and high quantum yield. Instead what is special is the Ligand-to-Metal Energy Transfer (LMET) also called the "antenna effect" which could work as a detector for metal cations[27]. When using lanthanoids, you are working with high and flexible coordination numbers, this means it can be quite difficult to find suitable organic linkers and to design these MOFs to be stable[26].

2.5.1 Copper

Copper is one of the transition metal ions used in the thesis with an oxidation state of 2+. This oxidation state gives the possible coordination number 4, 5, and 6 with an ionic radius from 57-73 pm[28].

As for the incorporation of copper in MOFs, this together with silver is one of the more investigated metal ion within MOF structures in group 11. One of the famous copper MOFs is the HKUST-1 MOF which was early in the MOF territory displaying large surface area. In addition to that the MOF also proved to have exceptional gas storage capacity[29].

2.5.2 Cobalt

Cobalt is another metal that has been used in this thesis and it is in the ninth group. The two possible oxidation states are 2+ and 3+. In this thesis, the 2+ oxidation state is more likely the one that has been used. Cobalt has a then the possible coordination numbers of 4, 5, 6, and 8 leading to an atomic radius of 58-90 pm depending on the direction of spin[28].

Cobalt is the most studied metal within MOFs in group 9 due to the properties that can be achieved in those MOFs, like a MOF being magnetic[29].

MOF synthesis made by Francoise Noa et al. where they used cobalt and the H_6cpb created the MOF CTH-9, which created the **yav**-net topology[22].

2.5.3 Zinc

The metal zinc can be found in group 12 and is the only metal in this thesis which is not a transition metal or a lanthanoid. Zinc is of the oxidation number 2+ and has a coordination number of 4, 5, 6, and 8. For the chloride salt, it is believed to be 4 and for the nitrate salt, it is believed to be 6 using the mercury software. With the possible coordination numbers zinc would then have an ionic radius of 60 pm respectively 74 pm[28].

Zinc is one of the primary metals in group 12 that is used in MOF studies. The metal is the basis for the formation of zeolitic imidazolate frameworks. These frameworks helped to discover liquid MOFs which appeared by melting these frameworks[29].

Zinc MOFs have been made with one of the organic linkers used in this project, H_6cpb, this combination of the organic linker and metal was synthesized by Francoise Noa et

al. They created three different MOFs with zinc ions. Two were called CTH-11 and Zn-MOF-888 which both had the **kgd**-net topology and the third MOF was called CTH-13 and had the **yav**-net topology[22].

2.5.4 Aluminum

Aluminum has the oxidation number 3+ which makes it suitable for trigonal bonding which is desired in this thesis. The coordination number of aluminum depends on the salt it is bonded to, in the case of $AlCl_3 \cdot 6H_2O$ it is believed to be 6. The ionic radius of aluminum would then be around 53.5 pm[28].

Aluminum is in group 13 in the periodic table and has been a material to use for MOF synthesis for a long time. Aluminum became prominent in this group since it allows for some of the MOFs to have "breathing" properties. This means the MOF can have both large and small pores which makes the MOF flexible in its structure which is beneficial[29].

2.5.5 Vanadium

Vanadium belongs to group 5 in the periodic table and has multiple possible oxidation states of 2+ all the way to 5+. In this thesis, the 3+ oxidation state is believed to occur. The coordination number for vanadium is then possible to be believed to be 6 with an ionic radius of 78 pm[28].

Once again the metal of choice, vanadium, is the most common material in its group when it comes to the synthesis of MOFs. The MOFs that have been synthesized have varying topologies. The vanadium MOFs come with different properties depending on the topology. To name some, there have been MOFs that have permanent porosity and there are also MOFs that have shown good separation properties of xylene isomers[29].

2.5.6 Manganese

Manganese is in group 7 in the periodic table with an oxidation state of 2+ and more. In this thesis the believed state would be 2+ leading to the possible coordination numbers of 4-8. Looking at the crystal of the manganese salt in mercury 6 would be the estimated coordination number. With different spins, the ionic radius can be 67 pm for low spin and 83 pm for high spin[28].

Manganese 2+ has been used in MOFs previously. One of the functions for it has been to be interchangeable with zinc in MOF structures. This makes it interesting to compare them in this thesis. Manganese MOFs are primarily synthesized through post-synthetic metalation. Post-synthetic metalation is when you add the desired metal onto an already existing framework exchanging the metal basis of the MOF[29].

2.5.7 Zirconium

In group 4 zirconium can be found which is believed to have the oxidation state of 4+. The possible coordination numbers for a zirconium ion with oxidation state 4+ ranges from 4 to 9. This would mean the ionic radius for the investigated zirconium ion is somewhere between 59 pm and 89 pm[28].

MOFs have as previously mentioned had some trouble with application in the real world due to stability issues. Zirconium is one of the elements which has proven to create stable MOFs. The UiO series of MOFs from the University of Oslo demonstrated a large surface area while still being stable under rough conditions in 2008[29]. What makes the MOFs with zirconium more stable is the high oxidation state of 4. This high oxidation state allows for stronger bonding between the carboxylate groups and the zirconium ions. If not a stronger bonding there is at least a higher attraction towards each other which facilitates bonding[15].

2.5.8 Terbium

Terbium is a metal in the lanthanoids f-block. It has an oxidation state of 3+ which would lead to the coordination numbers of 6, 7, 8, and 9 to be possible. This would then mean the ionic radius would be between 92.3 pm and 109.5 pm[28].
Lanthanoids in MOFs and terbium especially have luminescent properties which have led to the synthesis of mixed lanthanoid MOFs. A MOF with terbium and europium was made which could change its color depending on temperature. Lanthanoids are useful in MOFs due to their high amount of different coordination numbers leading to new structures[29].

Terbium MOFs have the possibility to shine light visible to the human eye with only the aid of a UV lamp[30]. This makes it possible for them to have simpler applications like forensic lights. This property will be tested in the thesis.

2.5.9 Gadolinium

Gadolinium is believed to be a 3+ oxidation state in this thesis as it would fit better with the organic linkers. With that oxidation state, Gadolinium has the possible coordination numbers of 6, 7, 8, and 9 which can give an ionic radius between 93.8 pm and 110.7 pm[28].

Gadolinium is like terbium, a lanthanoid, and possess the general properties of the lanthanoids like high coordination numbers. Gadolinium ions are highly paramagnetic[31], which means MOFs with gadolinium could be utilized in current magnetic resonance imaging contrast agents[32]. Gadolinium ions have a preference in binding to negatively charged atoms as the oxygen in carboxylate ligands[32]. The fact that they have this preference makes them a viable choice for binding to the ligand used in this thesis.

2.6 Potential end-product of MOF synthesis

2.6.1 CO_2 and I_2 adsorption

MOFs and similar molecules like COFs and organic polymer crystals have shown promising results in another application area where they work as "breathing" molecules. This means that there is a certain amount of flexibility in the molecule. This allows for ions, cations, and molecules to be packed in these structures within the voids which can increase in volume (breathing mechanism) as molecule uptake occurs. The ability to pack molecules

within the structure causes MOFs to function as containment and absorbent to certain molecules, with possible applications in CO_2 and I_2 adsorption.

An application for these properties is also found in the nuclear chemistry area where the radioactive isotopes ^{129}I and ^{131}I are common to occur. Here, MOFs could work as a vessel for these isotopes. Therefore, the ability for MOFs to catch and contain isotopes can be investigated through I_2 adsorption in a ToF-SIMS or simply by adding I_2 to a closed vessel and let it absorb onto the MOF[22].

Using the same premise, there is still a need for better exhaust control and specifically CO_2 containment to lower greenhouse gases. The same idea is applicable here, that the MOFs could capture and contain the CO_2 molecules in a more efficient way than what is used currently. There is also the possibility to create MOFs which could catalyze the formate synthesis from CO_2 instead of just capturing it[33].

2.7 Solvothermal synthesis

Solvothermal synthesis is a simple synthesis method where control of, to a limited degree due to self-assembly, morphologies in structured materials such as metal oxides, and in the case of this thesis, MOFs. Solvothermal synthesis is performed in a closed vessel, like a vial or an autoclave system. The vessel is used in order for the reaction mixture to be able to work in temperatures above the boiling points of the solvents, the metal ions, and the organic linkers that are used in MOFs[34]. This is because of the closed vessel used in the solvothermal synthesis allows for autogenous pressure to increase[35].

In solvothermal synthesis the temperature and pressure are increased through heating of solvents above their boiling point, this makes for an increase in solubility and reactivity[36]. These properties make for a suitable environment to create MOFs as even though some of the metal ions and organic linkers might not be soluble. The environment set by the experimental procedure makes the reactions happen without the need for an excess amount of solvents. The solvents used in the thesis experiments are there to dissolve organic linkers and metal ion powder (N,N-Dimethylformamide (DMF)) and to facilitate Lewis acid-base reactions without bonding to the carboxylic acid on the linker (Acetic acid (AcOH)/Formic acid (FA)).

2.8 X-ray diffraction

X-ray diffraction operates in the fashion that x-rays are generated to create monochromatic radiation which is then aimed at the sample. The x-rays are generated by electrons from the outer orbitals of a metal, that has characteristic x-rays, moving into a lower energy state. When doing this transition the electrons produce and radiate x-rays characteristic for the metal. The x-rays created are aimed at the sample which reflects them by utilizing constructive interference which occurs when Bragg's law is satisfied. This can then be used to calculate the crystal lattice. Bragg's law:

$$n\lambda = 2d_{hkl}\sin(\theta_{hkl}) \tag{E.1}$$

Where n is the integer, λ is the wavelength of the x-rays, d is the interplanar spacing generating diffraction, and θ is the diffraction angle.

There are two main XRDs that determine structures of MOFs, PXRD, and SCXRD. Firstly, SCXRD will be used as it gives all the information needed about the structure of the MOFs being synthesized. But if a smaller crystal is synthesized that will not work in a SCXRD, then PXRD will be used to give as much information as possible.

SCXRD uses a solid single crystal from a sample to determine the structure. The result from a SCXRD analysis is more accurate as the peaks (reflections) are separated at a degree which makes the results easier to interpret and analyze. The downside of SCXRD is that a defect-free, large, solid crystal is needed. If such a crystal fails to be created PXRD is the next XRD analysis to try to investigate the crystalline structure of the material. In SCXRD the sample will be rotated by a goniometer so the crystal gets all selected orientations which will provide all needed data for structure analysis. The crystal is then lit up with a monochromatic x-ray source which will produce the diffraction pattern in different angles depending on rotation and incident beam angle. The SCXRD uses many 2D pictures to create a 3D picture of how the structure of the molecule looks by investigating the electron density within the crystal[37].

When the crystals are too small the PXRD is the next analytical method to use which also can be complemented with the sample-destructive method electron diffraction. In PXRD x-rays are aimed at the sample and are then diffracted from the sample. These reflections (diffractions) are analyzed by a detector that scans the sample for the whole angle of 2θ[38]. 2θ angles are gathered since that is what arises due to the random orientation of the powder that is analyzed[39].

A PXRD has three main parts in its setup, an x-ray, a sample holder, and a detector[40]. The mechanism of the PXRD is to analyze x-ray beams that has scattered off the sample which will provide diffraction peaks after analyzation by the detector. These peaks can be utilized with a reference to analyze the sample and possibly determining the compound[38]. Overall, PXRD structure analysis gets harder to do due to overlapping peaks[41].

From the SCXRD and the PXRD, properties such as phase identification of the sample can be obtained using a reference and databases. It is also possible to get the unit-cell size and shape as well as its orientation[42]. The differences can be shown in table 2.1.

Table 2.1: The differences between SCXRD and PXRD, original table from Li et al[37].

property	SCXRD	PXRD
unit cell determination	easy	difficult
space group	easy	difficult
peak overlap	no	yes
information on sample	single particle	overall
structure solution	possible	possible with difficulties sometimes
size limitation	>1 µm	>50 nm

SCXRD is somewhat hard to utilize at all points due to the difficulties of synthesizing large enough crystal for it to be a valid method. Hence another method needs to be utilized

to look at the same properties as SCXRD but not with the high demands. Electron diffraction is one of the methods that has shown possibilities and been proven to work to some extent[41]. It has also been known that it is possible to perform crystal structure analysis with electron diffraction[43]. The drawback of electron diffraction is that it is a destructive method. There is a risk that the sample will burn and be destroyed which has been countered by technical solutions. For MOFs, the sample is perhaps not always destroyed but there is still a risk for damage from the electrons[44].

Electron diffraction works similarly like XRD but instead it uses electrons to obtain the diffraction pattern from the specific sample. This is usually done in a Scanning-Electron Microscopy (SEM) or a Transmission Electron Microscopy (TEM) where the electron diffraction is collected similarly to SCXRD where diffractions from many different angles are gathered. All this information can then be gathered and analyzed to create a crystal structure in three dimensions[45]. This is however not used to a greater extent due to the analysis of the data is not trivial so a high amount of knowledge in this area is needed to interpret the data[46].

In this thesis PXRD measurements will be done by a Small Angle X-ray Scattering (SAXS) diffractometer. This machine utilizes the x-rays scattering off the sample in question just like in PXRD. These x-rays are then analyzed by a detector and this data can be used to create the same data as PXRD. The measurements are made at, as the name suggests, low angles where the most characteristic peaks of MOFs are expected. By rotating the detector at different angles and having a second detector, a larger angle in total can be measured by merging data. This then gives you the same analytical range as in PXRD. The SAXS diffractometer will be used instead of PXRD as samples can be mounted on a sample holder and several small samples can be run at the same time as it is automatically adjustable.

The SAXS diffractometer used in the thesis can work as a PXRD machine with the possibility to look at large things such as cellulose fibers and nanoparticles. This machine is therefore well-equipped to analyze samples such as MOFs. The difference between SAXS and PXRD, PXRD basically is Wide Angle X-ray Scattering (WAXS), is where you put the detector. Do you place it small or wide with reference to the incident angle? If MOFs should be analyzed with SAXS or WAXS is up to debate but both are possible and WAXS is more common.

2.9 Thermogravimetric analysis

Thermogravimetry is performed with a thermogravimetry analyzer which analyses the weight loss of a sample as a function of time or temperature. These results can then give a good idea of how thermally stable the sample is[47]. The weight loss in the sample from heating and how it degrades is usually what is investigated[48]. TGA can also give the thermal performance of samples[49] as well as determine the composition of certain samples[50]. In the case of MOFs it is important to know parameters such as stability, from TGA, to understand the MOF and find suitable applications[51].

2.10 Infrared Spectroscopy

Infrared spectroscopy (IR) is an analysis method similar to near-infrared spectroscopy and Raman spectroscopy, where all three methods are vibrational spectroscopy. IR is used to determine the functional groups on a sample. The IR instrument sends infrared energy at a sample. The energy gathered causes vibrations characteristic for each functional group which then can be analyzed to decide the functional group[52]. Metal-ligand vibrations are hard to detect in IR. This is why functional groups are looked at instead, to see if metal-ligand bonds possibly could have formed[53].

The specific method used in the thesis, Attenuated Total Reflectance (ATR), is reflectional spectroscopy. ATR works by measuring the change in an IR beam that will alter its properties as it reflects against a crystal that the sample is mounted on. The IR beam is then analyzed by an IR detector where the data can be used to construct a sample curve of wavenumbers (cm^{-1}) against transmittance (%). ATR is very fast and simple which makes it an often-used method in research.

3
Methodology

3.1 Synthesis of MOFs

The synthesis of the MOFs started by turning on a heating plate that has a magnetic stirring and set the temperature to 120-140°C. The desired organic ligand (one or more) was weighed upon a filter paper and then added to a vial. The same procedure was performed for the metal salt. Then one half of the DMF was added and the mixture was stirred until a homogeneous mixture was achieved. AcOH and the other half of DMF were added to the mixture and stirred again to create a homogeneous mixture. When a homogeneous mixture had been achieved the liquid product was poured into a teflon beaker which then was put into an autoclave system. If a oven with a set time is not to be used the liquid could also be put into a microwave vial. The mixture is then heated and cooled until crystals are synthesized. The different heating programs can be found in appendix A3

3.2 Crystal extraction/Filtration

In this section, the different extraction methods used during the thesis will be described.

3.2.1 Crystal extraction/Filtration, funneling

To extract crystals from solutions the procedure was started with heating DMF in a vial to 120°C. The heating was done if the crystals are supposed to be extracted directly when they have been taken out of the oven. A filter paper was placed on a Buchner funnel or a funnel was created with the filter paper which was then placed on a beaker. The crystals are then washed with DMF firstly and then washed with dichloromethane (DCM) or methanol depending on what metal salt was used. Crystals were then collected from the filter paper. The sample was stored in the washing solution (DCM or methanol) due to the possibility of them being unstable in air.

3.2.2 Crystal extraction/Filtration, centrifuging

When the crystals are very small or require drying for them to be extracted, a crystal extraction with centrifugation is needed. The sample holder is centrifuged so the solids in the sample descend to the bottom of the sample holder.

3.3 Thermogravimetric analysis

TGA was performed in a Mettler Toledo DSCA/TGA 3+ with a continuous flow of air and the temperature was increased with 10°C/min from 30°C up to a total of 800°C.

3.4 SAXS sample pretreatment

The sample to be analyzed was dried to a powder and mounted upon a SAXS sample holder module. This was done by placing the sample on a microscopic glass with enough powder to cover at least a fourth of the sample holder which is a circle with 3mm in diameter. Then, by using a piece of scotch tape, the powder is extracted and placed in between to pieces of scotch tape. This assembly is then mounted so the sample is inside one of the circular sample spots on the module. The module is then put into the SAXS machine and the analysis of the material could commence. It is of importance that latex gloves are used during the entire procedure to prevent any fatty oils to be attached to the scotch tape and tamper with the results. Further, to not misinterpret samples, the same kind of scotch tape should be used through the entire experiment and other experiments that should be compared. It is of importance that only the two pieces of tapes are covering the sample and not a third piece of tape as this could affect the background noise differently just like changing the scotch tape could. More information about the SAXS machinery can be found in Appendix A2.

3.5 PXRD sample pretreatment

The sample to be analyzed is dried to a powder and mounted upon the sample holder of the PXRD machine. When the sample has been placed and the sample holder has been mounted in the XRD machine, a drop of ethanol is added to the sample for the sample to be sturdy during the analysis. To get reasonable results, there needs to be a circular sample with approximately 1-3mm in diameter, the larger the diameter the better results with less background noise.

3.6 ATR

Firstly, there is an ATR-module added to an IR spectrometer. The powder sample is then placed to cover the area of the sample holder required to collect viable data for a good measurement. The powder is pressed with the ATR crystal so that excess air in the sample is removed which would otherwise be shown as an error in the measurement. The measurement is then performed.

3.7 Mercury XRD powder pattern simulations

During the thesis a computer software called Mercury, from the CCDC, has been used[54]. This software was used to simulate estimated PXRD patterns for the potential MOFs that have been synthesized during the thesis. The procedure started with downloading the .cif file for a known MOF with a confirmed structure. This file was then opened in mercury

and the structure of the molecule and its data would then be in the software where it could be manipulated. An example is when the MOF called CTH-9, which is a cobalt MOF, was downloaded. In the structure of that MOF, the same organic linker as in this thesis was used so one could guess that a similar structure or the same structure could be possible for the metal chosen to work with. The cobalt metal ions in the structure were exchanged for whatever metal that was to be investigated. This then created the MOF CTH-9 but with another metal. Mercury then has a calculation device in which it can predict a PXRD pattern to be compared to the experimental PXRD data that was apprehended. If there are similarities then a similar or exact structure could be possible for the synthesized MOF.

4

Experimental

In this chapter, the methods and the number of materials used will be presented.

4.1 Synthesis of MOFs

For synthesizing the MOFs different molar ratios were evaluated. 1:2, 1:3, and 1:4 molar ratio between organic ligands and metal were tried for the experiments. If there were around 30 mg of powder, 2 ml of DMF and 2 ml of AcOH were used. If less or more was used, the amount was changed accordingly.

4.2 Synthesized MOFs and their recipes

This section describes what metal salts were used and how much of the salts were used. There is also information provided on what organic linkers were used and the amount.

The recipes of MOFs synthesized and produced during time period 1 (28th of January 2020 to 29th of February 2020) with a molar ratio of 1:2 (organic linker: metal salt) can be viewed in Table 4.1.

Table 4.1: The different MOFs prepared and the amount of metal salt and organic ligand. Solvent used for synthesis was DMF, AcOH and FA. An asterisk (*) at sample means it was heated and synthesized according to method 3.1 in the Memmert oven according to program description given to specific asterisk. If no asterisk they were made according to method 3.1 in a microwave vial.

Sample	Metal salt	Metal salt(mg)	H_6cpb(mg)	DMF(ml)	AcOH/ FA	solvent (ml)
VE-Tb1	$TbCl_3 \cdot 6H_2O$	14.96	16	2	AcOH	2
VE-Co1	$Co(NO_3)_2 \cdot 6H_2O$	11.9	16	2	AcOH	2
VE-Zn1	$ZnCl_2$	5.4	16	2	AcOH	2
VE-Al1	$AlCl_3 \cdot 6H_2O$	6.5	16	2	AcOH	2
VE-Co2	$Co(NO_3)_2 \cdot 6H_2O$	11.7	16	2	AcOH	2
VE-Zn2	$ZnCl_2$	5.6	16	2	AcOH	2
VE-Al2	$AlCl_3 \cdot 6H_2O$	6.3	16	2	AcOH	2
VE-V1(1*)	VCl_3	3.4	16	2	AcOH	2
VE-Mn1	$MnCl_2 \cdot 4H_2O$	7.94	16	2	AcOH	2
VE-Zr1	$ZrOCl_2$	13.05	16	2	AcOH	2

The recipes of MOFs synthesized and produced during time period 2 (19th of February 2020 to 17th of March 2020) with a molar ratio of 1:1.25:2 (H_6cpb: ppb: metal salt) can be viewed in Table 4.2. These samples were mixed using H_6cpb, ppb and different

transition metal ions in the first row. These samples were made with 2ml of DMF and 2ml of AcOH in total according to method 3.1.

Table 4.2: The different MOFs prepared and the amount of metal salt and organic ligand. The solvent used for synthesis was always 2 ml of DMF and 2 ml of AcOH. An asterisk (*) at sample means it was heated and synthesized according to method 3.1 in the Memmert oven according to program description given to specific asterisk. If no asterisk they were made according to method 3.1 in a microwave vial.

Sample	Metal salt(salt+mg)	H_6cpb(mg)	ppb(mg)
VE-Cu+ppb	$Cu(NO_3)_2 \cdot 3H_2O$ + 1.92	3.18	5
VE-Co+ppb	$Co(NO_3)_2 \cdot 6H_2O$ + 2.3	3.18	5
VE-Zn+ppb	$ZnCl_2$ + 1.1	3.18	5

The recipes of MOFs synthesized and produced during time period 3 (4th of March 2020 to 17th of March) with a molar ratio of 1:3 (organic linker: metal salt) can be viewed in Table 4.3.

Table 4.3: The different MOFs prepared and the amount of metal salt and organic ligand. Solvent used for synthesis was always DMF with AcOH or FA. An asterisk (*) at sample means it was heated and synthesized according to method 3.1 in the Memmert oven according to program description given to specific asterisk. If no asterisk they were made according to method 3.1 in a microwave vial.

Sample	Metal salt(salt+mg)	H_6cpb(mg)	DMF(ml)	AcOH/ FA	solvent (ml)
VE-Tb2(2*)	$TbCl_3 \cdot 6H_2O$ + 11.5	8	1	AcOH	1
VE-Gd1(2*)	$Gd(NO_3)_3 \cdot 6H_2O$ + 13.8	8	1	AcOH	1
VE-Zn3	$Zn(NO_3)_2 \cdot 6H_2O$ + 8.2	8	1	AcOH	1
VE-Al3	$AlCl_3 \cdot 6H_2O$ + 4.2	8	1	AcOH	1
VE-V2	VCl_3 + 5	8	1	FA	1
VE-Mn2	$MnCl_2 \cdot 4H_2O$ + 6	8	1	AcOH	1
VE-Zr2	$ZrOCl_2 \cdot 8H_2O$ + 9.9	8	1	AcOH	1

The recipes of MOFs synthesized and produced during time period 4 (26th of March 2020 to 10th of April) with a molar ratio of 1:4 (organic linker: metal salt) can be viewed in Table 4.5.

Table 4.4: The different MOFs prepared and the amount of metal salt and organic ligand. Solvent used for synthesis was always DMF with AcOH or FA. An asterisk (*) at sample means it was heated and synthesized according to method 3.1 in the Memmert oven according to program description given to specific asterisk. If no asterisk they were made according to method 3.1 in a microwave vial.

Sample	Metal salt(salt+mg)	H6(mg)	DMF(ml)	AcOH/ FA	solvent (ml)
VE-Al4(3*)	$AlCl_3 \cdot 6H_2O$ + 4.2	8	1	AcOH	1
VE-Zr3(3*)	$ZrOCl_2 \cdot 8H_2O$ + 9.9	8	1	AcOH	1

The recipes of MOFs synthesized and produced during time period 5 (11th of May 2020 to 22nd of May) with a molar ratio of 1:4 (organic linker: metal salt) can be viewed in Table 4.5.

Table 4.5: The different MOFs prepared and the amount of metal salt and organic ligand. Solvent used for synthesis was always DMF with AcOH or FA. An asterisk (*) at sample means it was heated and synthesized according to method 3.1 in the Memmert oven according to program description given to specific asterisk. If no asterisk they were made according to method 3.1 in a microwave vial.

Sample	Metal salt(salt+mg)	H6(mg)	DMF(ml)	AcOH/ FA	solvent (ml)
VE-Tb3(3*)	$TbCl_3 \cdot 6H_2O$ + 56	30	6	AcOH	6

5

Results

In this section, the results for different MOFs created during different time periods will be shown. The results will be reviewed in groups of what metal was used, first all cobalt results then all terbium results, etc. The methods of analysis that will be reviewed are PXRD, TGA, IR, and luminescence testing.

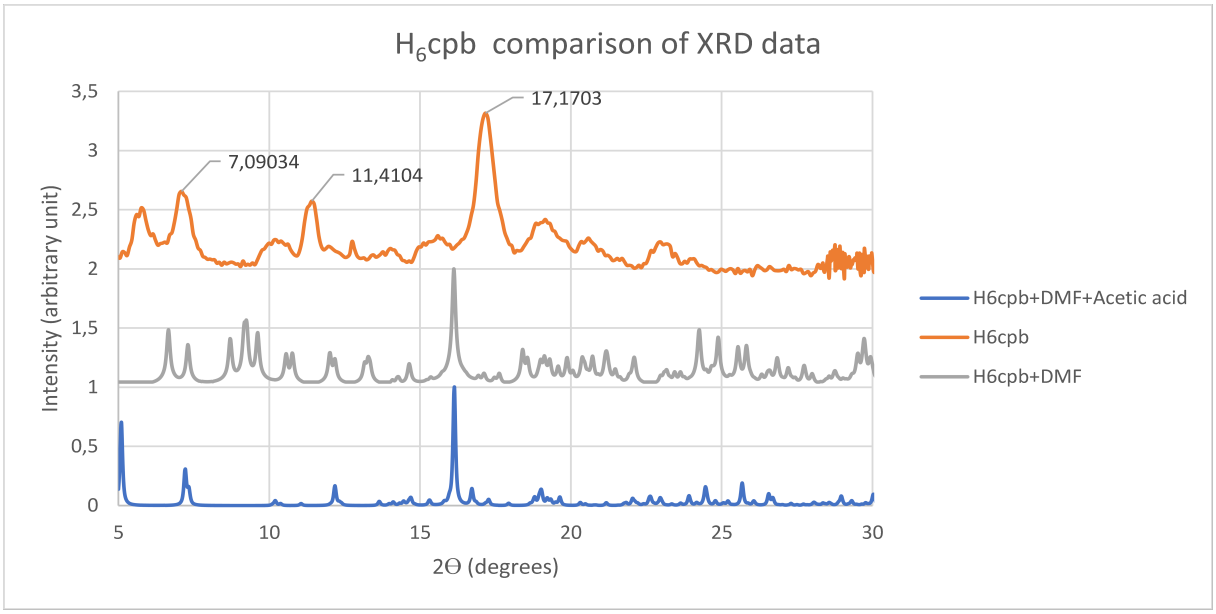

Figure 5.1: PXRD data of a H6$_{cpb}$+DMF+AcOH crystal, H6$_{cpb}$+DMF crystal and H6$_{cpb}$ powder, where the two samples in blue and grey are unpublished work by Dr Francoise Noa

Figure 5.1 shows what it looks like if the organic linker has not synthesized into a MOF with the metal but rather crystallized on its own with DMF. This image will be used to look at different PXRD data and conclude if there is a reaction with the metal ion in the metal salt or if self-crystallization of the linker and DMF has occurred. There is both the H_6cpb+DMF in a crystalline state and the H_6cpb in powder form as well as the H_6cpb with DMF and AcOH. The most important peak symbolizing if there is crystalline H_6cpb with DMF is the large peak at 16.6 which means that the H_6cpb has self-crystallized instead of bonding with the metal salt in the desired way. But there can also be seen some reoccurring peaks at 7 and 11. The orange H_6cpb line is run in a SAXS diffractometer compared to the other two, which were run in a PXRD.

The peaks showing in the graph, and the graphs to come, visualize that there is at least some degree of crystallinity due to the reflections which give peaks. Using Bragg's law, it can be calculated that the peak at 11 means there is a lattice spacing of 8.4 Å and

the peak at 7 gives a lattice spacing of 14.2 Å. This spacing would then be somewhere in the unit-cell or in between different cells. After reviewing these distances on previous MOFs made with H_6cpb and their structures these distances could be explained through the software mercury. 8.4 Å is thought to be the lattice spacing of a molecule (possibly metal) binding to the center hexagon of the H_6cpb molecule. The distance of 14.2 Å is thought to be the distance of the H_6cpb molecule from side to side which means there is H_6cpb in the sample but not in a self-crystalline state.

If peaks occur between 5 and 16 degrees this means something has reacted with the metal salt that has a larger lattice spacing than the H_6cpb in a self-crystalline state. Since metal salts should have a lower lattice spacing (higher degrees are where the metal ions are thought to be) the peaks at lower degrees can be assigned to the linker in MOF formation.

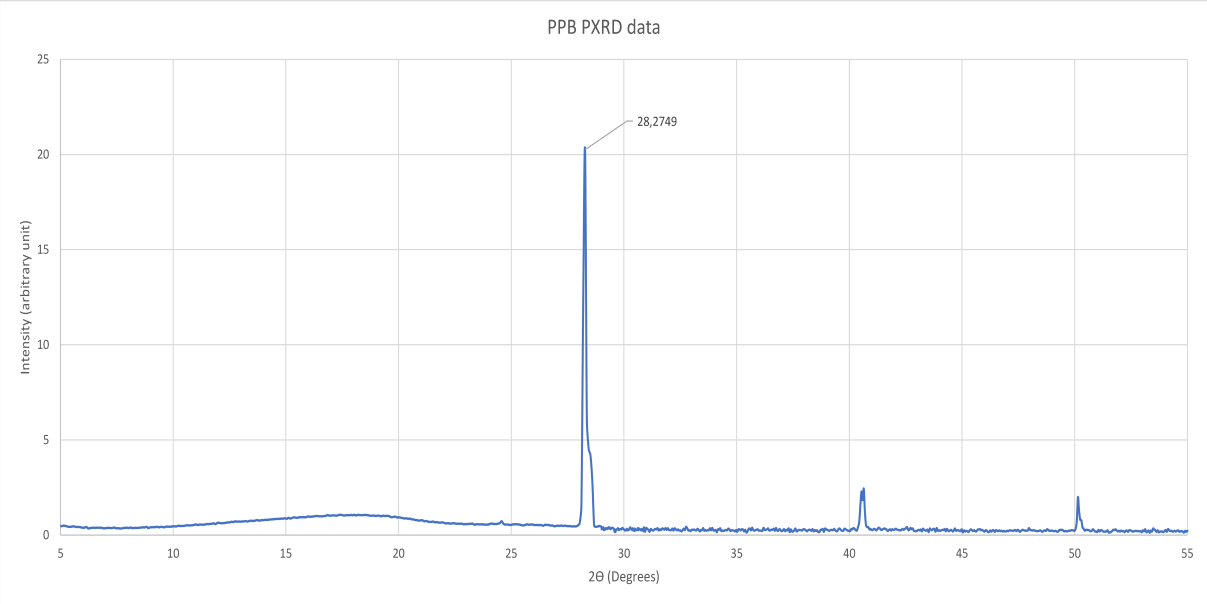

Figure 5.2: PXRD data of a the ppb linker in powder form.

Furthermore, Figure 5.2 shows the ppb in powder form to evaluate the metal salts paired with ppb, this sample was analyzed in a SAXS diffractometer.

5.1 Copper

A metal that was used in the smaller part of the project utilizing the ppb linker was copper. One sample was made and the synthesis results can be seen in Table 5.1.

Table 5.1: The MOF samples are reviewed in terms of what observations were found during synthesis. There is also mentioned if there where crystal created with a yes or no followed by a yes or no if the crystal was large enough to analyze with SCXRD. Lastly, an indication of how long the sample was in the oven.

Sample	Observations	Crystals	Suitable SCXRD	Time in oven
VE-Cu+ppb	black smudge	YES	NO	23 days

As with all the experiments with the organic linker ppb the ratio of 1:1.25 H_6cpb:ppb was used. This was to make sure that the combination would react together to form the new

system. The copper sample did not crystallize well as the crystals were small and looked more like black mud in its appearance and consistency. The supernatant was stored in new vials for further reaction in the oven but nothing happened. Crystal extraction was then performed which can be seen in Table 5.2.

Table 5.2: The table shows what solvent was used to wash the crystals and if the product was suitable for PXRD.

Sample	Washing solvent	PXRD
VE-Cu+ppb	Methanol	NO

During the crystal extraction all sample was lost in the filter paper probably due to the small size of the crystals. It was due to this problem the method described in section 3.2.2 was introduced to the thesis. However, this made further analysis of the copper sample impossible.

5.2 Cobalt

In this section observations of the cobalt sample will be reviewed.

Table 5.3: The MOF samples are reviewed in terms of what observations were found during synthesis. There is also mentioned if there where crystal created with a yes or no followed by a yes or no if the crystal was large enough to analyze with SCXRD. Lastly, an indication of how long the sample was in the oven.

Sample	Observations	Crystals	Suitable SCXRD	Time in oven
VE-Co1	Dry pink crystals	YES	NO	17 days
VE-Co2	Cloudy pink crystals	YES	NO	12 days
VE-Co+ppb	black smudge	YES	NO	27 days

The cobalt samples with only the H_6cpb linker had some crystals but as they were copies of previous laboratory work performed by Francoise Noa et al[22], they were not investigated with SCXRD. These samples were instead cross-referenced by doing PXRD in a SAXS diffractometer.

In the experiment with ppb the sample was very wet and amorphous and did not crystallize well. The black smudge when investigated with a microscope was however thought to be crystalline but with very small crystals.

The supernatant of the sample was stored in a new glass vial and was further placed in the oven to see if further crystallization could occur. This was not successful.

Crystal extraction was performed for the two samples VE-Co1 and VE-Co+ppb were the results can be viewed in table 5.4

Table 5.4: The table shows what solvent was used to wash the crystals and if the product was suitable for PXRD after extraction.

Sample	Washing solvent	PXRD
VE-Co1	DCM	YES
VE-Co+ppb	Methanol	YES

Both samples were extracted but with different methods. VE-Co1 was crystalline enough to use filter paper with the normal method described in section 3.2.1 while the VE-Co+ppb was extracted according to section 3.2.2. Crystal extraction and further analysis of sample VE-Co2 was not performed since VE-Co1 had then already been analyzed and they were replicas of each other.

VE-Co1 was investigated with PXRD and the results can be seen in Figure 5.3.

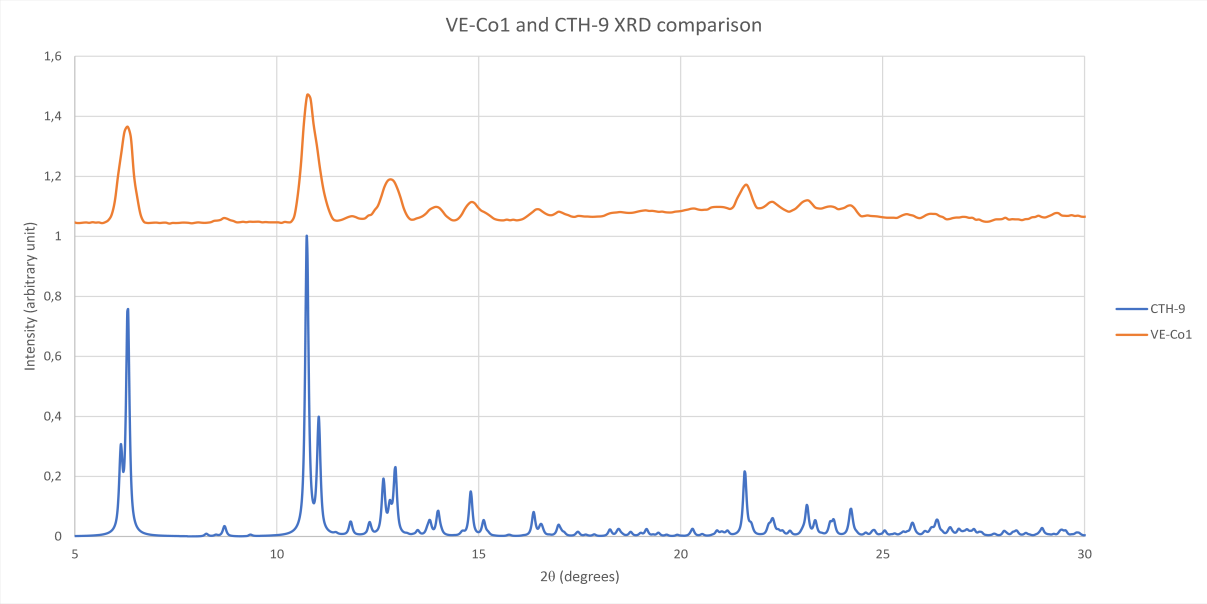

Figure 5.3: Comparison of PXRD data between VE-Co1 and CTH-9 synthesized by Francoise Noa et al[22]. Where CTH-9 is simulated by mercury

The two samples VE-Co1 and CTH-9 (the old cobalt MOF) have the same characteristic peaks but with different intensity. Intensity is of less importance due to it being an arbitrary number. This means that this PXRD is a good indication of that MOF CTH-9 has been replicated. The CTH-9 PXRD data was simulated and apprehended through the software mercury.

The cobalt sample made in combination with the linker ppb was cross-reference with another sample with the same linker. This sample was made from nickel and is unpublished work by Francoise Noa et al. The comparison can be viewed in Figure 5.4.

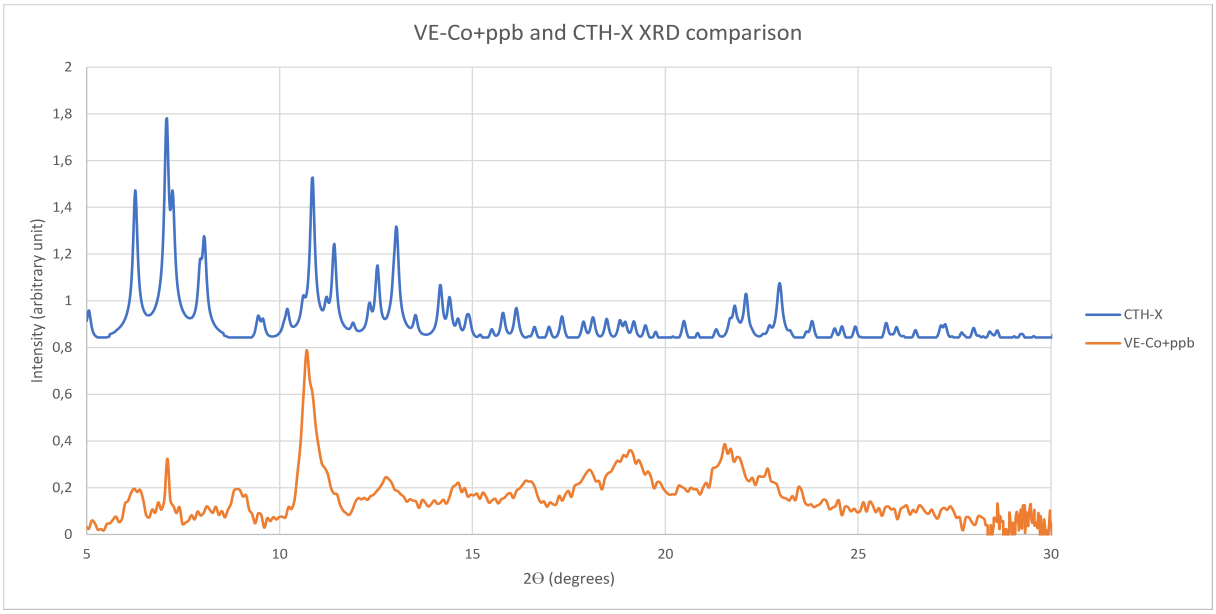

Figure 5.4: Comparison of PXRD data between VE-Co+ppb and CTH-X synthesized by Francoise Noa et al. The data of CTH-X is simulated by mercury and is unpublished results.

There were two characteristic peaks, 7 and 11, which indicates that a reaction has occurred. However, the two samples are not matching as the VE-Co+ppb lacks a lot of the peaks visible in the simulated pattern of CTH-X. However, it can be seen that something has happened as the sample is not similar to the references of the different linkers H_6cpb and ppb when considering their respective PXRD-results.

When it comes to the comparison in PXRD, between CTH-X and VE-Co+ppb, it is visible that there is not much resemblance other than some small peaks. From the PXRD comparison we cant conclude if they have similar topology or not. The XRD data of CTH-X was simulated and apprehended through mercury.

The nickel sample had hexagon crystals and when the cobalt sample was investigated in a microscope it also had hexagon crystals. A comparison between the two crystals can be seen in Figure 5.5.

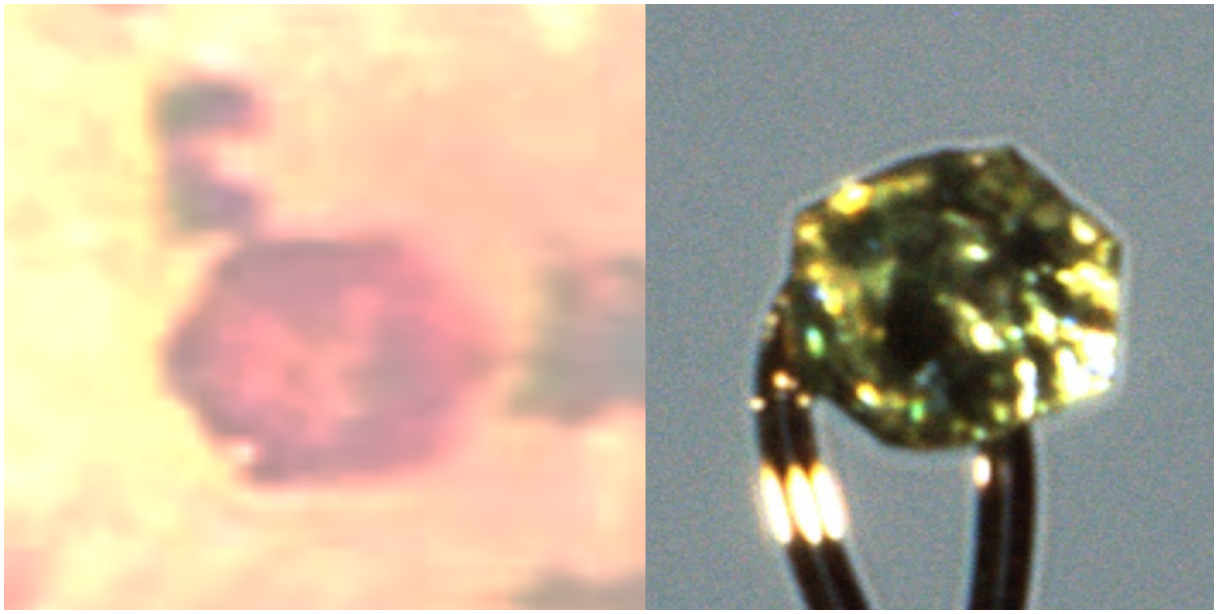

Figure 5.5: Comparison of the two crystal made with the linker ppb. VE-Co+ppb to the left and CTH-X synthesized by Francoise Noa et al.[22] to the right.

The sample VE-Co+ppb was due to this microscopic visual very interesting and was sent for further evaluation of the crystal in Germany.

5.3 Zinc

Four samples of zinc were made during the thesis and 2 of the samples (VE-Zn2 and VE-Zn+ppb) got lost in the process and could not be analyzed with PXRD, TGA, or IR.

Table 5.5: The MOF samples are reviewed in terms of what observations were found during synthesis. There is also mentioned if there where crystal created with a yes or no followed by a yes or no if the crystal was large enough to analyze with SCXRD. Lastly, an indication of how long the sample was in the oven.

Sample	Observations	Crystals	Suitable SCXRD	Time in oven
VE-Zn1	Salt like flakes	YES	NO	17 days
VE-Zn2	No crystals	NO	NO	28 days
VE-Zn3	White powder	YES	NO	>30 days
VE-Zn+ppb	black smudge	YES	NO	27 days

VE-Zn1 successfully yielded crystals, a picture of the microscope investigation can be seen in appendix A5. The other samples with successful crystal synthesis were VE-Zn3 and VE-Zn+ppb. The VE-Zn2 sample did not yield any crystals and could not be further analyzed. Crystal extraction was then performed on the successful samples and information can be found in Table 5.6.

Table 5.6: The table shows what solvent was used to wash the crystals and if the product was suitable for PXRD.

Sample	Washing solvent	PXRD
VE-Zn1	DCM	UNKNOWN
VE-Zn3	DCM	YES
VE-Zn+ppb	Methanol	YES

When the crystals were washed it was discovered that DCM could potentially dissolve the crystals if the metal salts where chlorides. This was discovered as VE-Zn1 was dissolved when washed and the crystals disappeared. This was then utilized for other metal ions and the main washing solvent after this event became methanol. Due to the small size of the crystals in VE-Zn+ppb the same centrifugation method was used as for the VE-Co+ppb sample. For both the VE-Zn3 sample there were crystals formed which could be analyzed with PXRD before there was no sample left to perform TGA or IR.

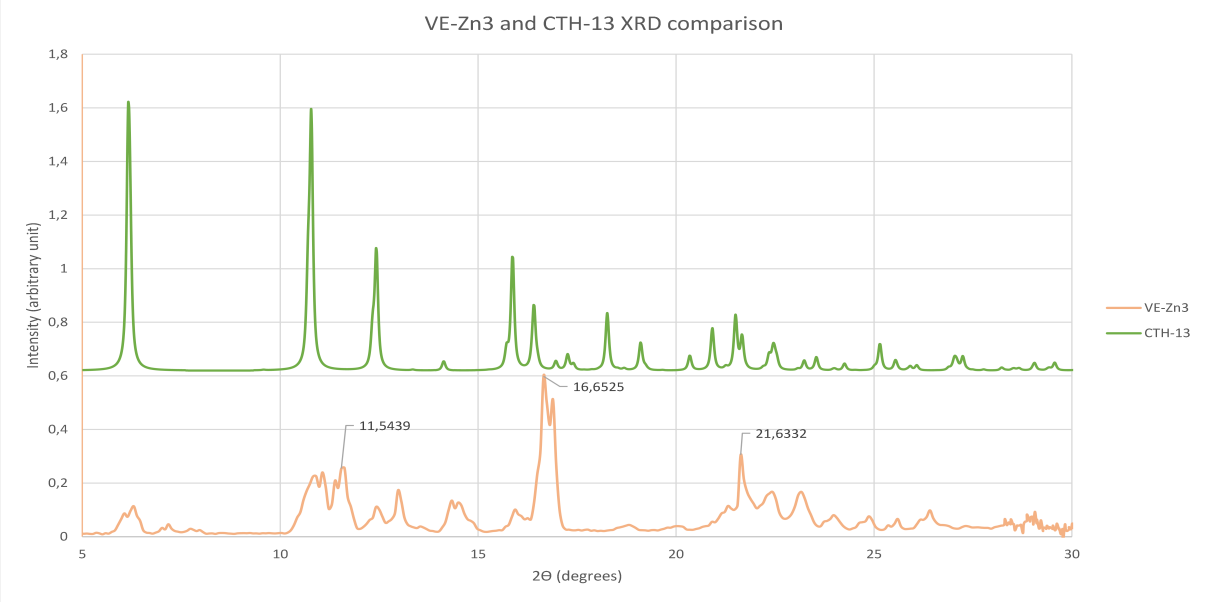

Figure 5.6: Comparison of the VE-Zn3 PXRD data to CTH-13. The data for CTH-13 were provided from Francoise Noa et al[22]. The CTH-13 data was simulated and apprehended through the software mercury.

In Figure 5.6 many peaks can be noticed. One peak is the mentioned 16 peak which would indicate that this could be H_6cpb that has crystallized with itself and DMF. Comparing this graph to Figure 5.1 some similarities can be seen but not too many. Hence, there could be a MOF with the zinc ion but there is also self-crystallized H_6cpb and with the lack of clear peaks the most probable result is that there is no MOF but rather an impure zinc complex. Similar to the other samples there are new peaks between 5 and 16 degrees indicating some form of reaction as well as the standard peaks at 7 and 11.

In the figure there is also a comparison of the PXRD data from a zinc MOF (CTH-13) synthesized by Francoise Noa et al[22]. It can be seen that there are similarities towards the higher degrees but in the case of the VE-Zn3 sample, the largest and most prominent peak is the one at 16 degrees, H_6cpb self-crystallization. While for the CTH-13 MOF there are two large peaks at around 7 and 11 which as mentioned before could indicate that there is a bond between H_6cpb and a metal ion. These two peaks are not present at a prominent level in the VE-Zn3 sample. The XRD data for CTH-13 was simulated and apprehended through mercury.

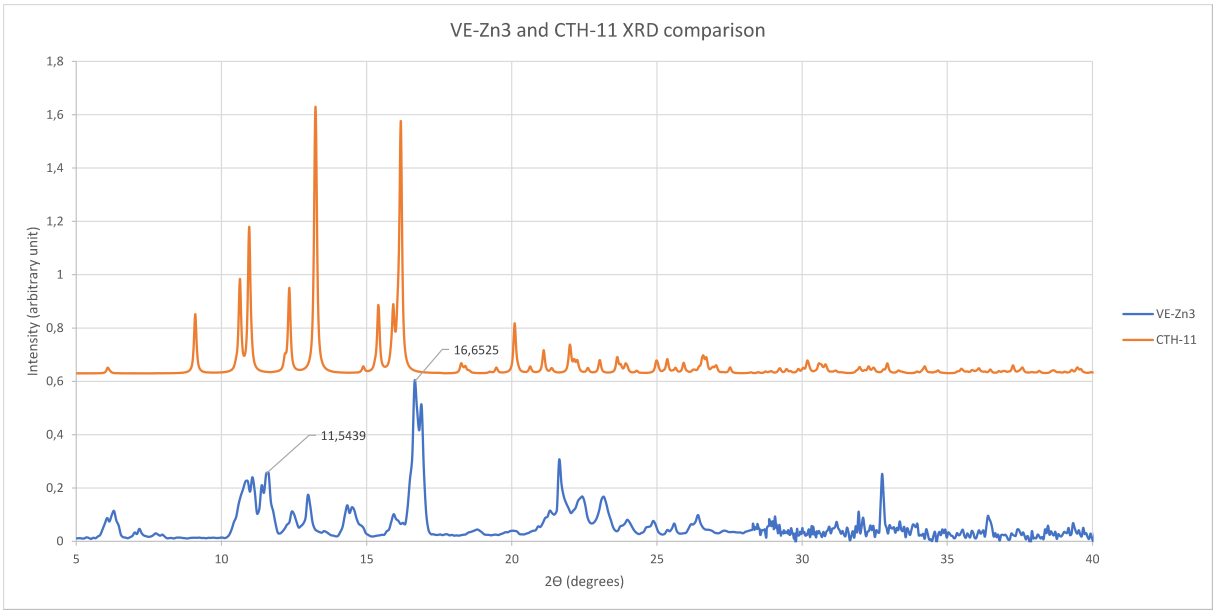

Figure 5.7: Comparison of the VE-Zn3 PXRD data to CTH-11. The data for CTH-11 were provided from Francoise Noa et al[22]. The data for CTH-11 was simulated and apprehended through the software mercury.

Another comparison to a zinc MOF can be seen in Figure 5.7 where the VE-Zn3 is compared to CTH-11. Here, a better overlapping of graphs but still lacking the core peaks. The 7 peaks from 10-17 degrees in the CTH-11 MOF can be assigned to 7 peaks in the VE-Zn3 sample but this is not something that is for certain as the offset is too big for it to be a good approximation. However, as before the 7 and 11 peaks are very small in VE-Zn3. The XRD data for CTH-11 was simulated and apprehended through mercury.

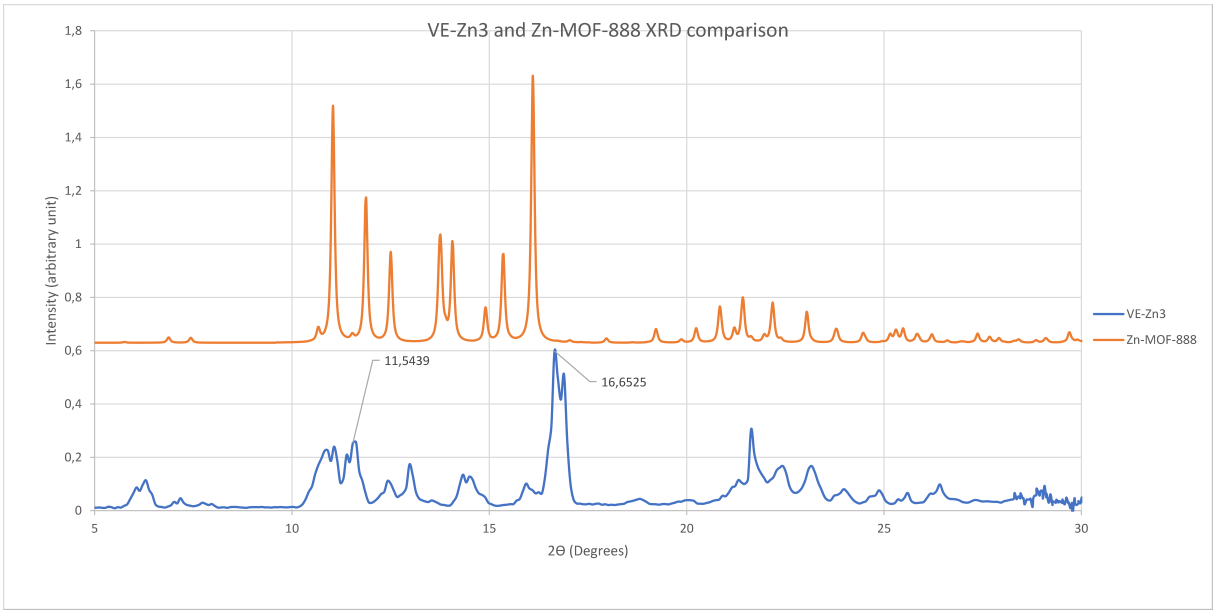

Figure 5.8: Comparison of the VE-Zn3 PXRD data to Zn-MOF-888. The data for Zn-MOF-888 were apprehended from Francoise Noa et al[22]. The data for Zn-MOF-888 was simulated and apprehended through the software mercury.

When the zinc sample is compared to another MOF mentioned in the work done by Francoise Noa et al[22] called Zn-MOF-888 something more comparable is found. It is clear in Figure 5.8 that there are more similarities than compared to the other zinc MOFs and

that maybe the VE-Zn3 sample could be a MOF of this character. The peaks are, as mentioned previously, not very clear but the peaks between 10 and 17 can once again be assigned to another peak in the VE-Zn3 sample with a bit of offset. However, the lack of fit in the curves is still too large for a conclusion that VE-Zn3 is a MOF. To conclude if it is a MOF or not, even though it is the best fitting of the zinc MOFs, can be done. The XRD data for Zn-MOF-888 was simulated and apprehended through mercury.

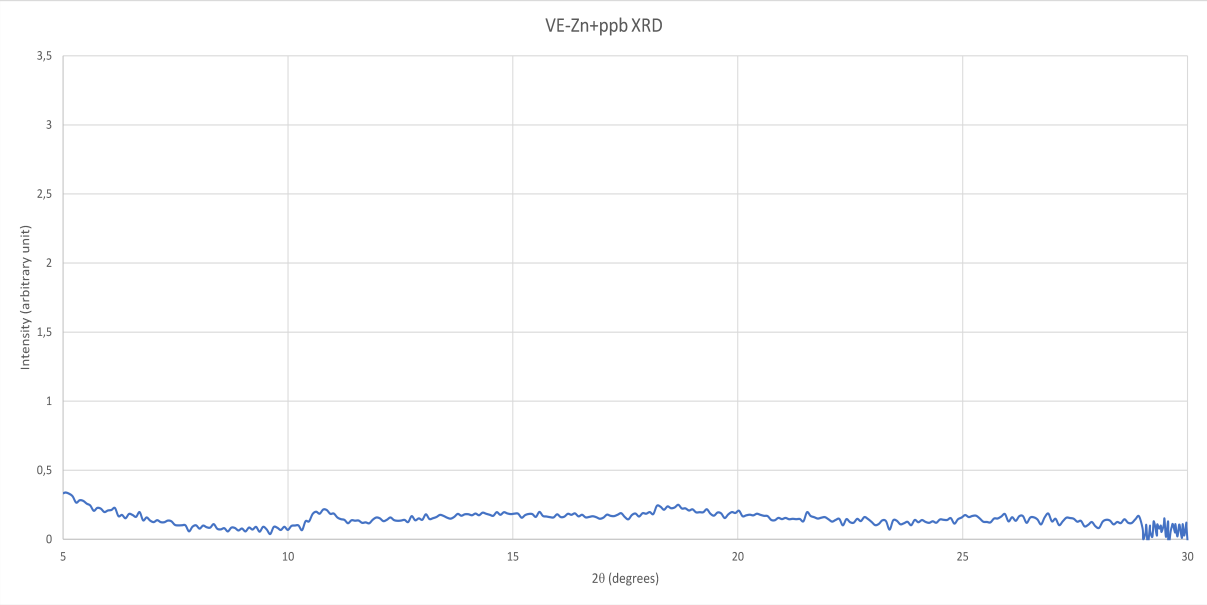

Figure 5.9: PXRD data of the VE-Zn+ppb sample.

Lastly, for the zinc sample in Figure 5.9, the zinc sample with the ppb linker, there are not a lot of peaks. This would indicate an amorphous material and there is very little, if any, crystallization of the sample.

5.4 Aluminum

Four samples of aluminum were made during the thesis and all of them produced some form of precipitate which was either crystalline or amorphous.

Table 5.7: The MOF samples are reviewed in terms of what observations were found during synthesis. There is also mentioned if there where crystal created with a yes or no followed by a yes or no if the crystal was large enough to analyze with SCXRD. Lastly, an indication of how long the sample was in the oven.

Sample	Observations	Crystals	Suitable SCXRD	Time in oven
VE-Al1	Dried salt/gel on glass	YES	NO	17 days
VE-Al2	Dried salt/gel on glass	YES	NO	12 days
VE-Al3	Dried salt/gel on glass-wall	YES	NO	9 days
VE-Al4(2*)	UNKNOWN	UNKNOWN	UNKNOWN	14 days

The first three samples of aluminum created a gel-like precipitate on the glass of the reaction vials. When the samples VE-Al1 and VE-Al3 had been synthesized, these were inspected through a microscope. Images of this can be found in the appendix, Figure A3 and Figure A4, were it is visible that they both have some crystalline parts and

some amorphous parts. The dried salt/gel is also visible as flakes in Figure A3. Crystal extraction was then performed on the samples VE-Al1 and VE-Al3 as the VE-Al2 did not look promising when studied in a microscope. For the sample VE-Al4 crystal extraction could not be formed due to the autoclave in which the sample was prepared broke and the sample could not be retrieved. The reaction was performed in an autoclave as a countermeasure to the observed affinity of the precipitate to the silica in the glass. Crystal extraction information can be found in Table 5.8.

Table 5.8: The table shows what solvent was used to wash the crystals and if the product was suitable for PXRD.

Sample	Washing solvent	PXRD
VE-Al1	Methanol	YES
VE-Al3	DCM	YES

For the aluminum sample VE-Al1, a large amount of sample could be retrieved from the wall of the glass vial. The sample did however not look crystalline and more like a gel. The gel could be dried and made suitable for PXRD analyzation. The same procedure could be adapted to the VE-Al3 sample. PXRD could then be performed on both of the samples which can be seen in Figure 5.10.

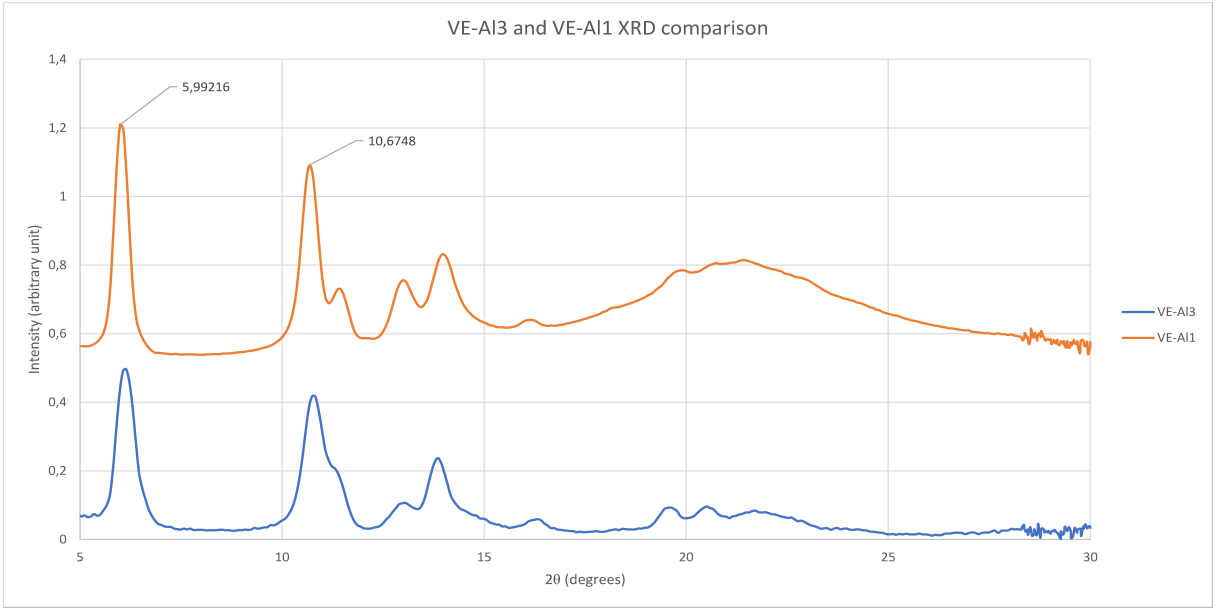

Figure 5.10: PXRD data for VE-Al1 and VE-Al3.

In this graph of the aluminum samples the two peaks around 7 and 11 are visible which could mean there is H_6cpb and something bonded to it, probably the aluminum ion. As with previous samples it cannot be guaranteed to be a MOF, but the peaks mean there is some crystalline material and that it is with H_6cpb. However, when it comes to the aluminum sample the observations made from the synthesis make the crystallinity of the sample questionable. It is visible, as with the other samples, that there are new peaks different from Figure 5.1 between 5-16 degrees which indicates a reaction between the H_6cpb and the metal salt. Further analysis would be needed to make a more solid statement if these are MOFs or not.

It is visible that even though the samples did not look that similar in the microscope, the created samples have similar structures due to their PXRD similarities.

5.5 Vanadium

Two samples of vanadium were made during the thesis where one of them yielded crystalline material and could be further analyzed.

Table 5.9: The MOF samples are reviewed in terms of what observations were found during synthesis. There is also mentioned if there where crystal created with a yes or no followed by a yes or no if the crystal was large enough to analyze with SCXRD. Lastly, an indication of how long the sample was in the oven.

Sample	Observations	Crystals	Suitable SCXRD	Time in oven
VE-V1(1*)	White crystals	YES	NO	1*+1 day
VE-V2	Green amorphous crystals	YES	NO	8 days

The white crystals found in the sample VE-V1 were not the same color as the original color of the sample, which was green, and as the sample was heated it turned blue. The white color of the crystal is thought to be the crystallization of the organic linkers together with DMF. The sample was then put back into an oven where the crystals then disappeared and did not re-occur, confirming that it was organic linkers that had self-crystallized with DMF as these are less thermally stable.

The green crystal found in VE-V2 was believed to be amorphous after microscopic investigation. Since a substantial yield was achieved, crystal extraction was performed to evaluate the sample with PXRD the information on crystal extraction can be found in Table 5.10.

Table 5.10: The table shows what solvent was used to wash the crystals and if the product was suitable for PXRD.

Sample	Washing solvent	PXRD
VE-V2	Methanol	YES

Crystals where successfully extracted and could be analyzed with PXRD. There was however not enough sample for any other tool of analysis. PXRD data analysis can be seen in Figure 5.11.

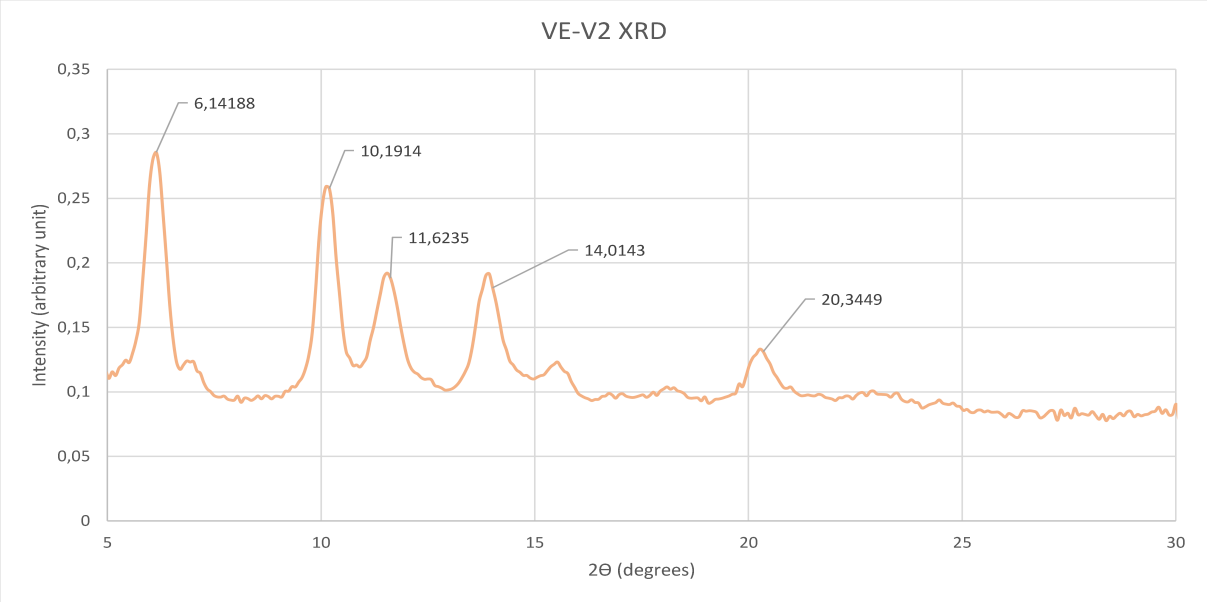

Figure 5.11: PXRD data of the VE-V2 sample.

In the figure, the same peaks as mentioned before at 7 and 11 can be seen. These are not as exact as before but it could be because they have a slight offset. There are other peaks which, just like in the aluminum sample. This could be a good result meaning it is a more crystalline sample and a MOF compared to the previous zinc comparisons. But because the meaning of these peaks are hard to interpret it could also be impurities of some sort. The trend continues as for previous samples and there are still new peaks between 5 to 16 degrees indicating a reaction between the metal salt and H_6cpb.

5.6 Manganese

Manganese samples were prepared during this thesis. This reaction was the best synthesis at producing precipitate and 2 samples where made. Both samples yielded crystalline material and could be further analyzed. This is represented in Table 5.11.

Table 5.11: The MOF samples are reviewed in terms of what observations were found during synthesis. There is also mentioned if there where crystal created with a yes or no followed by a yes or no if the crystal was large enough to analyze with SCXRD. Lastly, an indication of how long the sample was in the oven.

Sample	Observations	Crystals	Suitable SCXRD	Time in oven
VE-Mn1	Snowflake crystals	YES	YES	12 days
VE-Mn2	Small crystals	YES	NO	7 days

The manganese samples looked like white snowflakes but under a microscope they looked like tiny fibrils gathering in a pile which can be seen in the appendix Figure A7 for the VE-Mn1 sample. The crystal was very small but there were some larger parts of it so it could be a mix of MOF and self-crystallized H_6cpb. Both samples had crystals hence crystal extraction was performed which can be seen in Table 5.12.

Table 5.12: The table shows what solvent was used to wash the crystals and if the product was suitable for PXRD.

Sample	Washing solvent	PXRD
VE-Mn1	Methanol	YES
VE-Mn2	Methanol	YES

For VE-Mn1 the crystalline manganese powder had to be cross-referenced with PXRD of H6 crystals to ensure that it is not organic linkers that have crystallized with the solvent. This sample was sent to Stockholm for further investigation in SCXRD and electron diffraction. After being reviewed in Stockholm this sample was not able to be analyzed properly by their SCXRD and no specific results were apprehended from there. Not all of the sample was sent to Stockholm and PXRD was utilized on the sample that was left seen in Figure 5.12

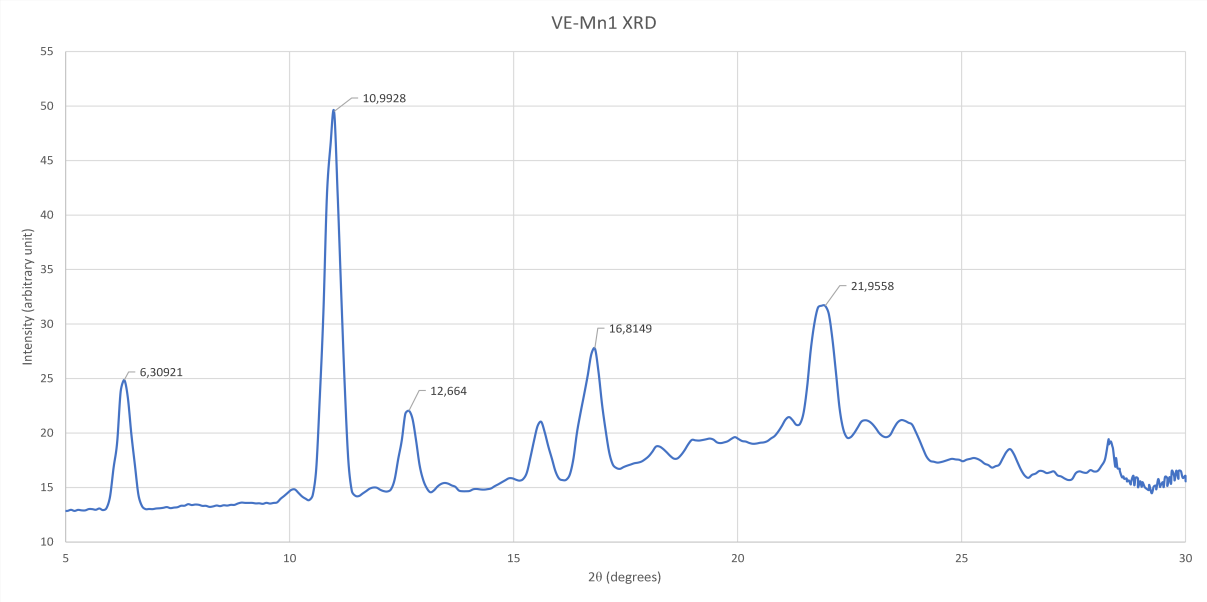

Figure 5.12: PXRD data of VE-Mn1.

The peaks around 7 and 11 are present again which could mean that there is something bonded to the H_6cpb but in this sample there is also the peak at 16.8 which could indicate H_6cpb self-crystallization. As mentioned previously, the sample was sent to Stockholm for further analysis.

Manganese powder was very easy to synthesis in larger quantities and therefore some of the VE-Mn2 powder was used for TGA before it was sent to Stockholm for it to be analyzed.

The VE-Mn2 was analyzed with TGA and the results are shown in Figure 5.13.

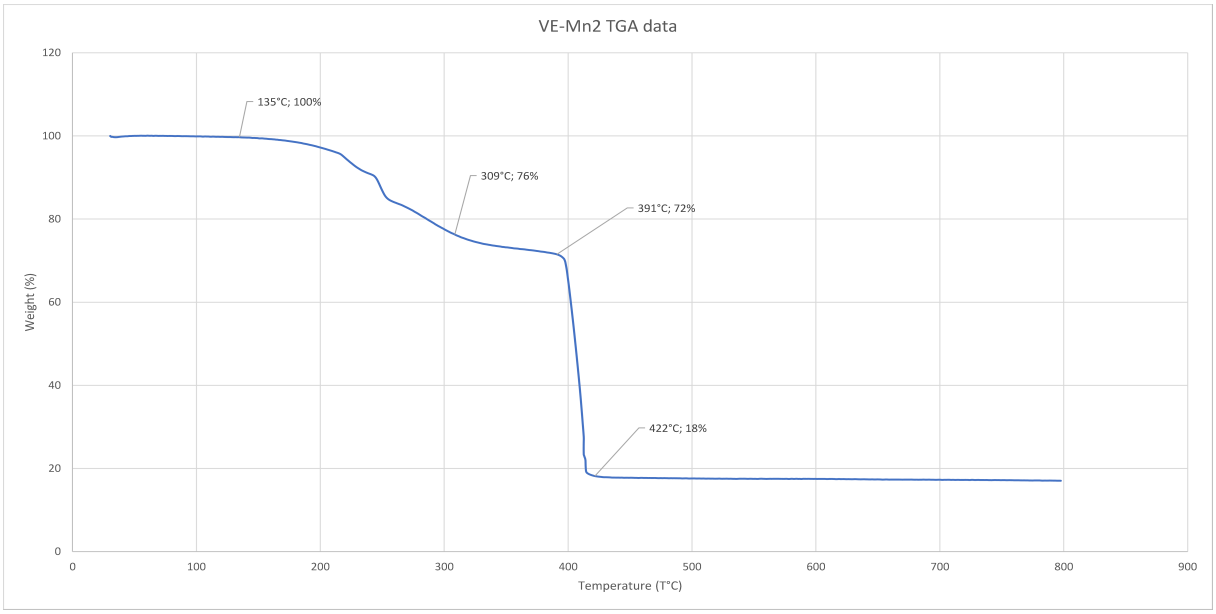

Figure 5.13: Plot of the VE-Mn2 sample after analyzation with TGA

In Figure 5.13, the VE-Mn2 has some information that can be gathered. The solvents that were left in the MOF have evaporated between the two points of 135°C and 309°C which was around 25-20% of the sample weight. The linker gets oxidized and burnt away between 391°C and 422°C which stands for about 53% of the sample weight. These temperatures using the organic linker H_6cpb is similar to the TGA analysis performed by Francoise Noa et al[22]. The resulting weight is thought to be manganese oxide which is around 18% of the sample weight. After calculations were made this then resulted in around 7% manganese in the sample. These calculations also stated that there is a 1:1.6 mole ratio of the linker to metal.

If the ratios of the different compounds would be known together with the structure of the presumed MOF, calculations would confirm if the structure was achieved. The weight could then be analyzed to see if the amount of manganese left in the sample was representative of a manganese MOF with that kind of structure. With the current information an estimate of the structure in regard to the weight left after the TGA could not be performed. A rough approximation can be done and calculations of it will be done only on the sample VE-Tb3 later in the results in Figure 5.21.

5.7 Zirconium

Zirconium was another metal used and it behaved similarly to aluminum in terms of the observations made during synthesis. The results of the synthesis with zirconium can be found in Table 5.13.

Table 5.13: The MOF samples are reviewed in terms of what observations were found during synthesis. There is also mentioned if there where crystal created with a yes or no followed by a yes or no if the crystal was large enough to analyze with SCXRD. Lastly, an indication of how long the sample was in the oven.

Sample	Observations	Crystals	Suitable SCXRD	Time in oven
VE-Zr1	Dry powder, burnt	YES	NO	12 days
VE-Zr2	White powder on glass	YES	NO	9 days
VE-Zr3(2*)	White crystals	YES	YES	14 days

Burnt samples, like VE-Zr1, was going to be done a second time to see if improvements could be made to ensure that they would not be burnt. The sample was not further analyzed. VE-Zr2 and VE-Zr3 are efforts of this.

VE-Zr2 started to grow as a layer on the glass vial it was synthesized in similarly to aluminum. The same change was applied to the zirconium sample as for the aluminum sample to prevent this and autoclave was used for another synthesis, VE-Zr3. The sample was nevertheless somewhat crystalline and crystal extraction was performed on both samples as VE-Zr3 also yielded crystals. The crystal extraction can be viewed in Table 5.14

Table 5.14: The table shows what solvent was used to wash the crystals and if the product was suitable for PXRD.

Sample	Washing solvent	PXRD
VE-Zr2	DCM	NO
VE-Zr3	Methanol	YES

For the first zirconium sample that was extracted much of the crystal was lost in the filter paper since very small amounts could be extracted from the glass vial. This problem could be due to the samples being quite amorphous and sticking to the wall of the vial. The small amount that was extracted was used to perform PXRD analysis.

The zirconium samples were more crystalline when synthesized in an autoclave system. This confirmed that the silica was interfering with the synthesis of a crystalline zirconium MOF. PXRD analysis was made and the two samples were compared which can be seen in Figure 5.14.

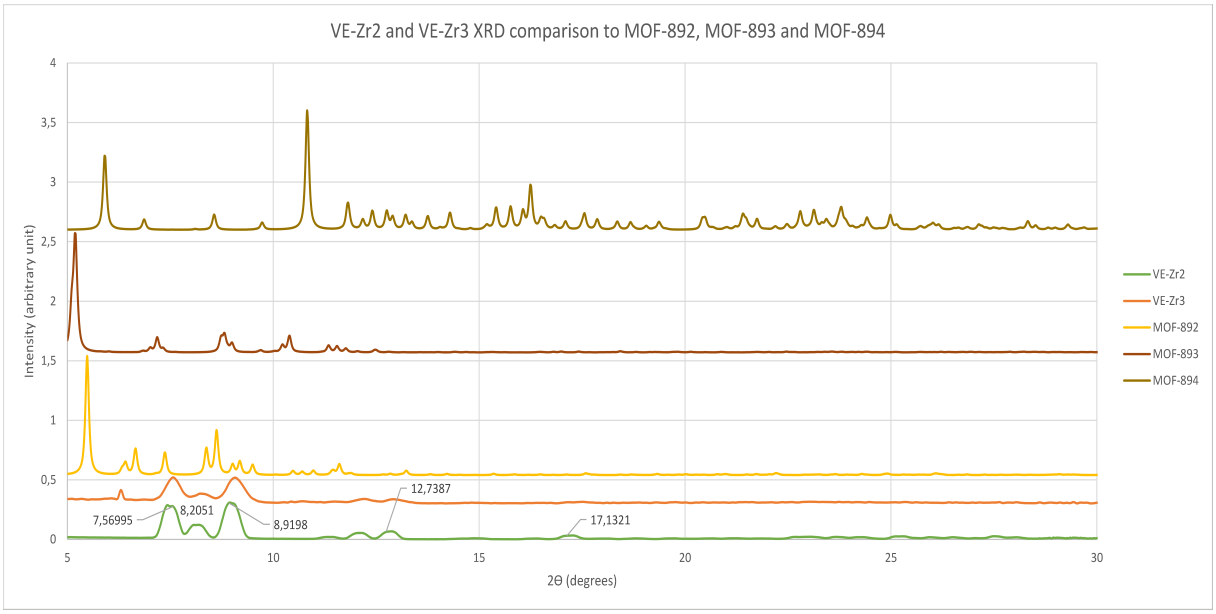

Figure 5.14: XRD data comparison of VE-Zr2, VE-Zr3 MOF-892, MOF-893 and MOF-894. MOF-892, MOF-893 and MOF-894 are all generated through the software mercury.

Considering Figure 5.14, there is reason to believe it is the peaks 7 and 11, but these are at lower angles in this figure. What these peaks means are not certain, but it can be concluded that a reaction has occurred as not any of the H_6cpb PXRDs have exactly these peaks or look similar. There are extra peaks below 16 which means a larger unit-cell has been created which is typical for MOFs.

VE-Zr2 was deemed a not viable sample due to its amorphous structure on the vial. It is however visible that the two samples are very similar with some extra peaks like the one at 6.3 in the VE-Zr3 sample. There are enough similarities to where it can be said that the reproducibility of this kind of MOF is feasible. That there is no peak at 6.3 could mean that there is a different size of unit-cell. This could indicate that the two samples have created different net topologies if they both did synthesize MOFs. They could also have very similar structures. To fully confirm any of these assumptions more structure analysis is necessary.

In the Figure there is also visual representation comparing the MOFs synthesized in this thesis to the work done by Nguyen et al[23]. It is visible that there is very little to no similarities. If any of these topologies are the same for VE-Zr2 or VE-Zr3 can not be concluded based on these XRD data comparisons. The plots for the work done by Nguyen et al was simulated and apprehended through the software mercury.

5.8 Terbium

MOFs were also prepared with some lanthanoid metal ions. Firstly terbium was used due to its interesting luminescent properties and three samples where made. The results for the synthesis can be seen in 5.15. The third sample was made due to the interesting PXRD shown for VE-Tb2 and now a larger quantity was desired to be able to analyze the sample with PXRD, TGA, IR, and UV-light.

Table 5.15: The MOF samples are reviewed in terms of what observations were found during synthesis. There is also mentioned if there where crystal created with a yes or no followed by a yes or no if the crystal was large enough to analyze with SCXRD. Lastly, an indication of how long the sample was in the oven.

Sample	Observations	Crystals	Suitable SCXRD	Time in oven
VE-Tb1	Dry powder, burnt	YES	NO	17 days
VE-Tb2(2*)	White powder	YES	NO	2*
VE-Tb3(3*)	White crystals	YES	YES	11 days

Burnt samples were to be synthesized a second time to see if improvements could be made to ensure that they would not be burnt. VE-Tb1 was not further analyzed. The other two terbium samples synthesized crystals and crystal extraction was then performed which can be seen in Table 5.16.

Table 5.16: The table shows what solvent was used to wash the crystals and if the product was suitable for PXRD.

Sample	Washing solvent	PXRD
VE-Tb2	Methanol	YES
VE-Tb3	Methanol	YES

There are numerous articles saying the terbium has luminescent properties just like some other lanthanoid metals like europium[55]. To see if this property was preserved after MOF synthesis, UV light was used. This was done for all samples to study their luminescence which can be seen in Figure 5.15 and Figure 5.16.

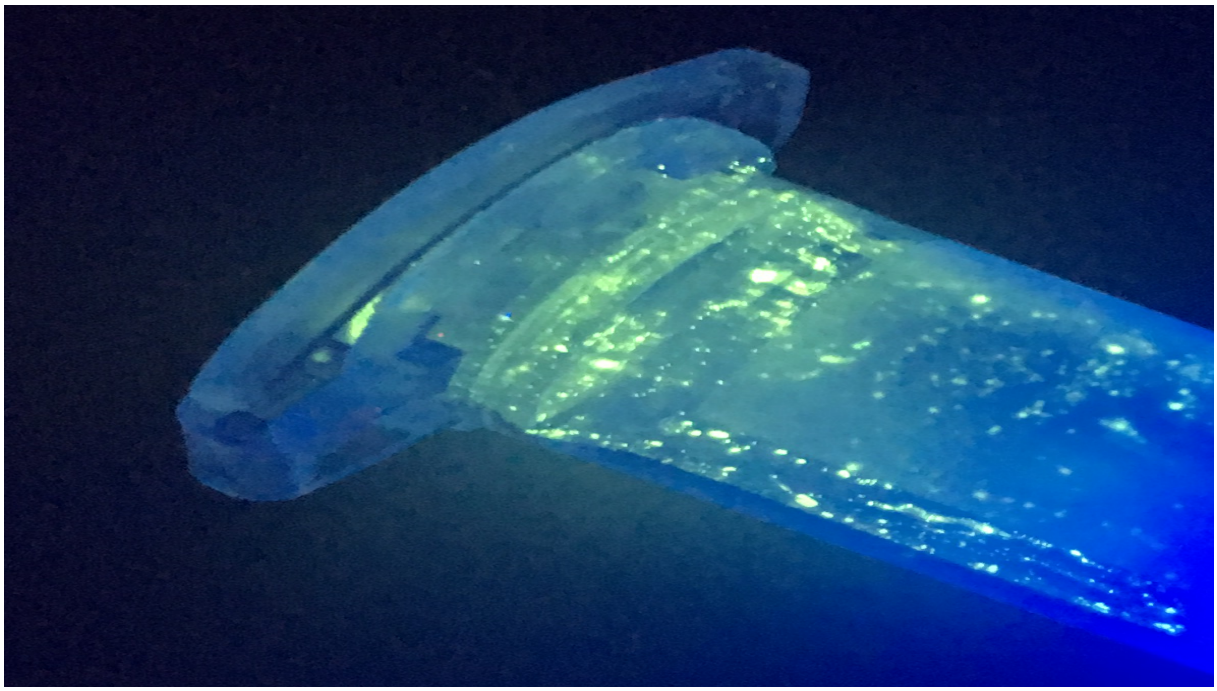

Figure 5.15: Photo of the VE-Tb2 sample under UV-light

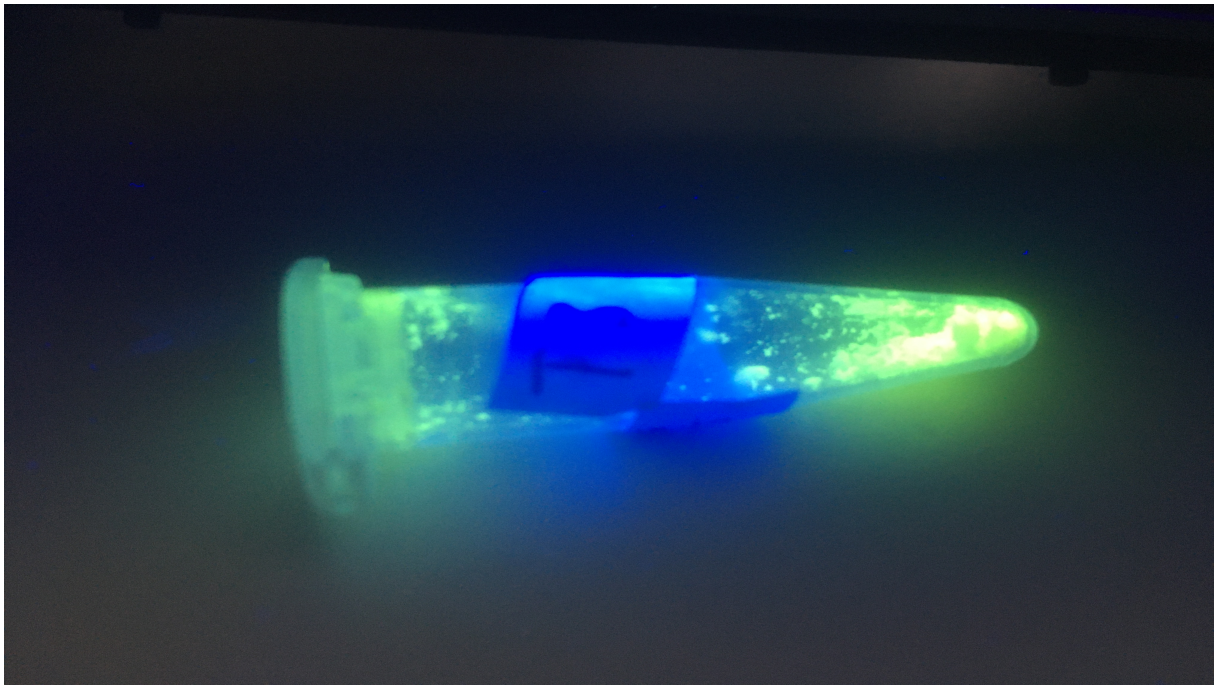

Figure 5.16: Photo of the VE-Tb3 sample under UV-light

As visible in the two figures of the terbium samples the luminescence property of terbium was preserved through synthesis. This could indicate together with the further analysis that the terbium is in the crystals and it is not only the organic linker. These UV-figures can be compared to the white sample of VE-Tb3 in the appendix Figure A2. PXRD was then utilized on both samples and compared which can be seen in Figure 5.17.

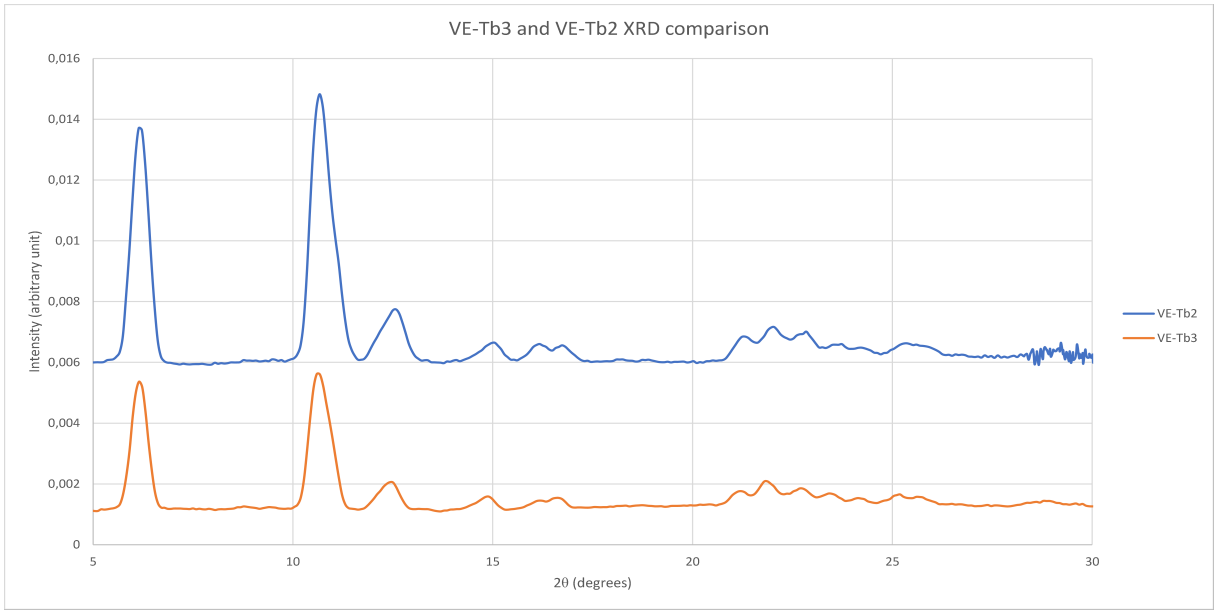

Figure 5.17: PXRD comparison of the data from VE-Tb3 and VE-Tb2.

In this PXRD data it can be confirmed that the same structure has been synthesized. There are two peaks at around 7 degrees and 11 degrees and then there are some small peaks from 12 to 30 degrees. The peak at 16 is not present and the sample does not in

any other way resemble self-crystalline linker. It can be estimated that a MOF has been formed but further structural analysis is needed, as for all promising samples.

To estimate a structure for VE-Tb3 in order to do TGA calculations, confirming the hypothetical structure, a PXRD was computer-generated. The PXRD was generated through the software mercury where the metal (in the loaded structure) was changed to terbium and a PXRD plot was apprehended. This was then used to see if there were any structural similarities and the best fit would be the estimated structure for the VE-Tb3. Different structures were tested but the best fit was with CTH-9 which is a cobalt MOF with the linker H_6cpb.

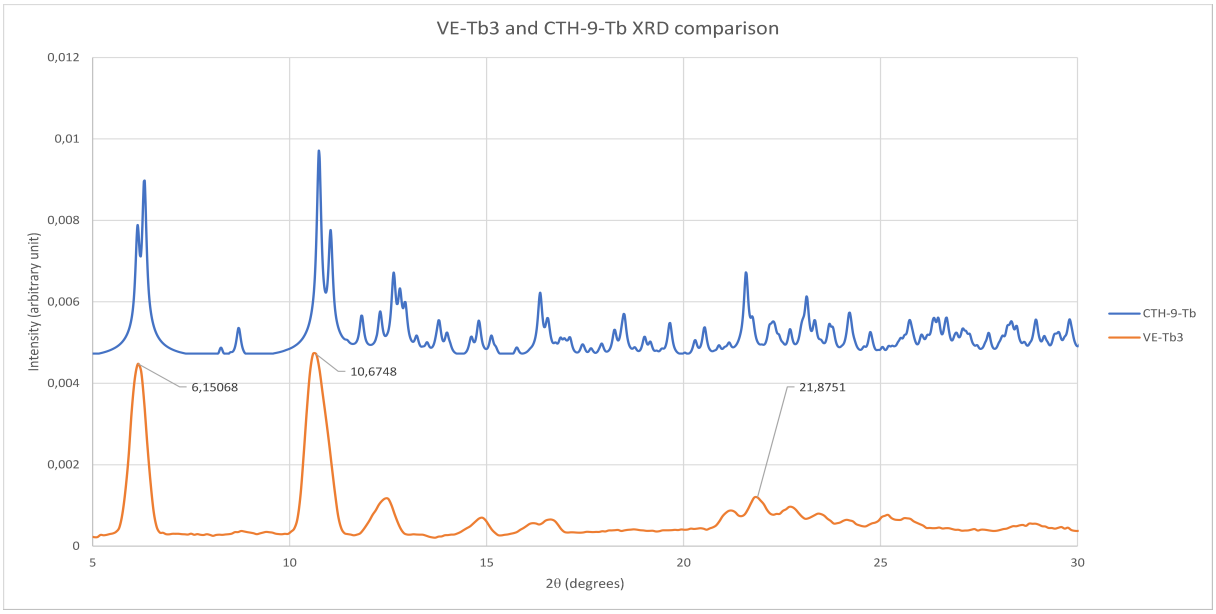

Figure 5.18: PXRD comparison of the data from VE-Tb3 with the generated PXRD data for a transformed CTH-9 MOF. The CTH-9-Tb was simulated and apprehended from the software mercury.

In Figure 5.18 it is visible that there are some similarities but not to any conclusive extent. The topology of the CTH-9 MOF, the **yav**-net, is probably not the correct topology but for the sake of the investigation this was the estimated structure.

Next step was to look at IR to see if any potential functional groups, primarily carboxylic acid, could be found indicating that a reaction had not occurred.

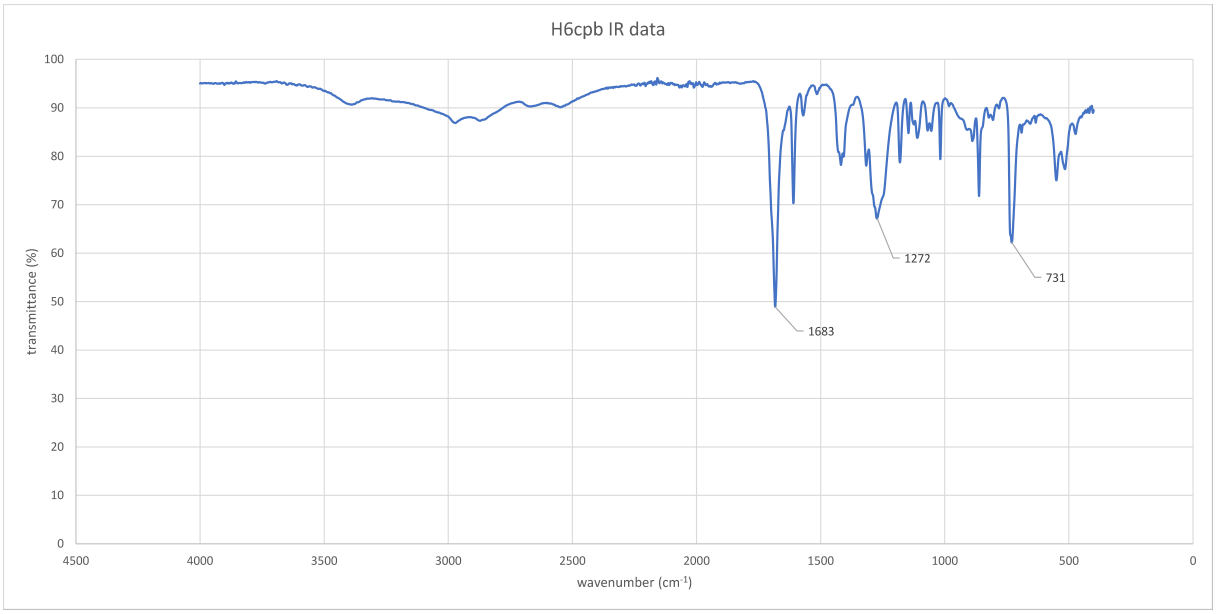

Figure 5.19: Plot of the organic linker sample after analyzation with IR

In Figure 5.19 data for the IR analysis of the organic linker H_6cpb can be seen. It can be seen there are three larger peaks but it is mainly the peak at 1683 that is characteristic for the H_6cpb powder and something to pay attention to in other IR spectra with potential MOFs. This peak is one of the carboxylic acid peaks (the main one) together with a broad peak at 3300-2500 and a sharp peak at 3500 which both would also indicate carboxylic acid. The peak at 731 could be some form of benzene derivatives from the linker.

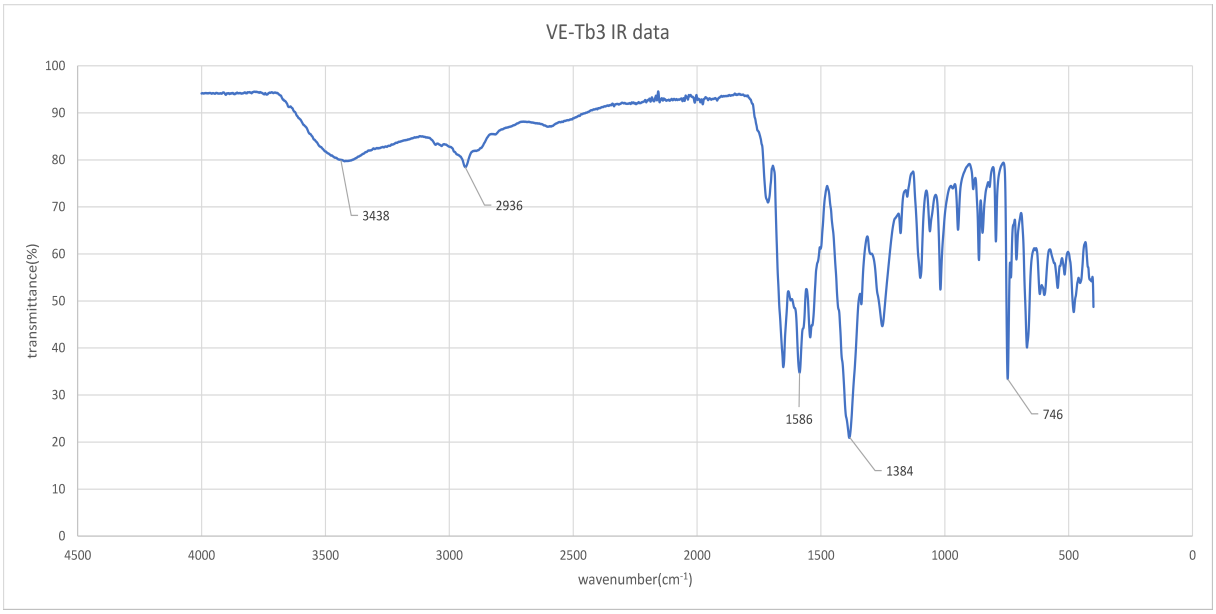

Figure 5.20: Plot of the VE-Tb3 sample after analyzation with IR

VE-Tb3 was analyzed with IR, this is represented in Figure 5.20. There is no peak at around 1700, indicating something has reacted with H_6cpb. The peaks 1586, 1384, and other peaks in that area are believed to be absorbed DMF when comparing to literature[56]. The peak at 746 is believed to be some form of benzene derivatives caused by the organic linker. The peak at 2936 could be C-H stretching in the organic linker. This figure

does however have a bulge at 3438 which could be the carboxylic acid bulge mentioned previously. The bulge could have some offset and the presence of it would then indicate that not all carboxylic acids have reacted. This would unreacted linker is in the sample indicating that a MOF might not have been synthesized. It could also mean that the sample is not homogeneous as the crystalline parts of the sample could be a MOF while there is extra organic linker.

The final step was to do calculations that depended on the TGA analysis. These calculations would show if the **yav**-net topology, which was estimated through mercury, was the correct topology. The TGA analysis can be seen in Figure 5.21

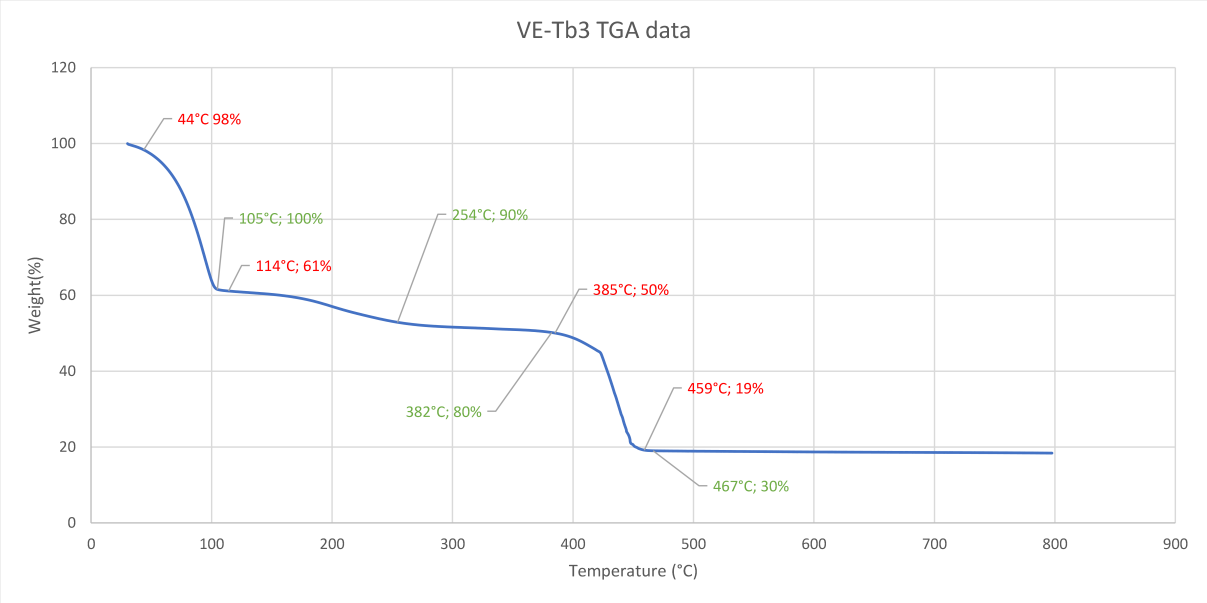

Figure 5.21: Plot of the TGA analysis of the VE-Tb3 sample

In the figure there is a large drop from 100% to 61% instantly with the numbers in red. This drop is thought to be extra solvents on the sample. The extra solvents could be there since the sample did not dry for a very long time before IR analysis was performed. The green numbers are then what is believed to be the data that can be evaluated.

Furthermore, there is a drop of 10% between 105 °C and 254 °C which would be the solvents evaporating from inside the crystals. There is then a drop from 90% to 80% where degradation of the organic linker occurs. Then a dip from 80% to 30% which is believed to be the burn-up of the organic linker and other organic materials. Left in the sample is 30 mass% which should then be terbium oxide. This TGA curve would then be typical to the TGA of other MOFs previously made the organic linker H_6cpb[22].

With all this data on the terbium sample, an estimation of the structure can be made based on CTH-9. Where there will be changes with chlorides instead of nitrates and terbium instead of cobalt. This would lead to the structure, [Tb4(cpb)(acetato)2(dmf)4Cl4], after balancing of charges with acetates and chlorides. This estimated structure would according to calculations retain about 81 weight% after solvent evaporation and linker degradation. This is similar to what was recorded in the TGA analysis. After the burn-up of organic linker the retained weight should be around 20% but during the TGA

analysis a weight percentage of 31% was achieved. This means there is an excess of something. This could be extra un-reacted terbium or some form of impurity but as this was just an approximation, the estimated structure could also just be wrong. Further structure analysis needs to be done with SCXRD in order to draw a definite conclusion if the VE-Tb3 adopted the **yav**-net topology.

5.9 Gadolinium

As the lanthanoid sample terbium showed interesting properties like luminescence and promising PXRD data another lanthanoid, gadolinium, was investigated. The synthesis of the gadolinium sample can be viewed in Table 5.17.

Table 5.17: The MOF samples are reviewed in terms of what observations were found during synthesis. There is also mentioned if there where crystal created with a yes or no followed by a yes or no if the crystal was large enough to analyze with SCXRD. Lastly, an indication of how long the sample was in the oven.

Sample	Observations	Crystals	Suitable SCXRD	Time in oven
VE-Gd1(2*)	White powder	YES	NO	2*

The white powder which looked crystalline was able to be synthesized. Crystal extraction was then utilized to look at PXRD and other methods of analysis if there was enough sample. Crystal extraction can be viewed in Table 5.18.

Table 5.18: The table shows what solvent was used to wash the crystals and if the product was suitable for PXRD.

Sample	Washing solvent	PXRD
VE-Gd1	DCM	YES

A substantial amount of gadolinium sample was able to be retrieved so that the sample could be analyzed by both PXRD and IR which can be seen in Figure 5.22 and Figure 5.23 respectively.

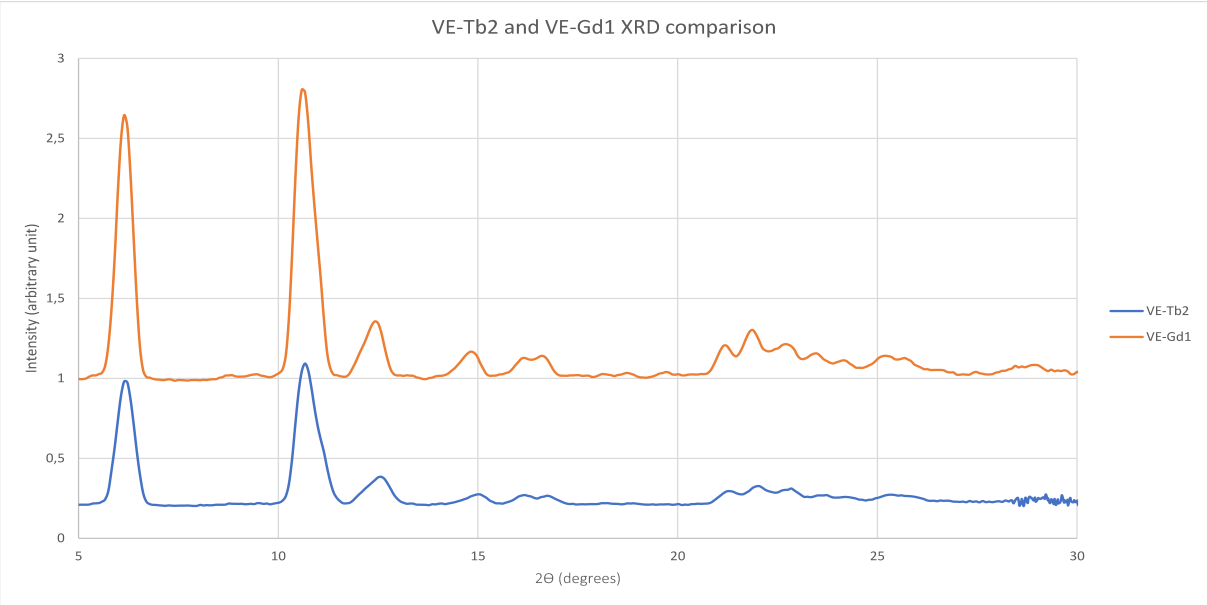

Figure 5.22: Comparison of the lanthanoids PXRD data. Lanthanoid samples in the graph are VE-Tb2 VE-Gd1.

The two typical peaks at 11 degrees and 7 degrees and the smaller typical lanthanoid peaks between 12 and 30 degrees can be seen in Figure 5.22. There is a lack of the H_6cpb peak and therefore it can be concluded that according to the PXRD analysis there is no self-crystallization of H_6cpb with DMF. Just like for the terbium samples it cannot be entirely concluded that a MOF has been synthesized due to the lack of analysis available.

A comparison of the two lanthanoids in this thesis can also be seen. They are very similar and have somewhat the same characteristic peaks at all degrees. That these two samples are so similar could indicate that they are iso-structural and have the same topology. The same observations for other lanthanoids have been seen in the parallel thesis by Axel Jonsson[57]. The remaining gadolinium was used for IR analysis shown in Figure 5.23.

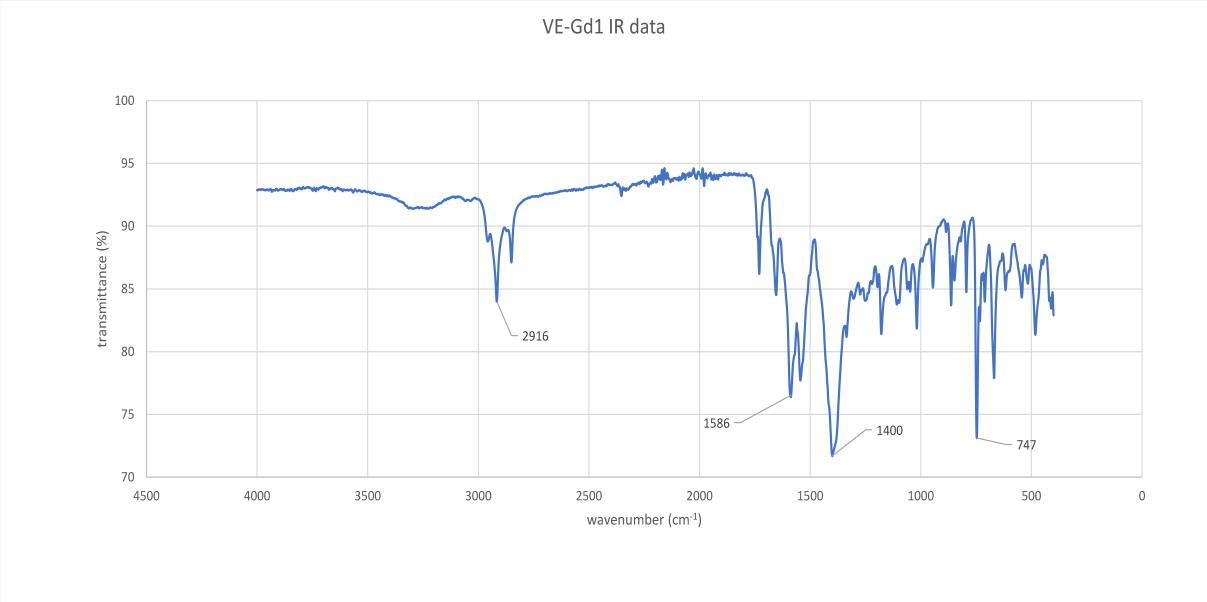

Figure 5.23: Plot of the VE-Gd1 sample after analyzation with IR

In the figure there is no visible peak at 1700 indicating a reaction has occurred. The peaks that in terbium was thought to be DMF is present in this sample as well as the benzene derivatives. The peak at 2916 is also there indicating C-H stretching in the linker. Differences like the bulge in the terbium sample not being visible in gadolinium could be that the sample has deprotonated over time. The gadolinium sample was analyzed with IR after a long time (since crystal extraction) compared to that of terbium.

6
Conclusion

The samples that were made during the thesis have, due to the COVID-19 virus, not been fully analyzed to look at crystal structures and deduce the net topology. Therefore, I cannot conclude if the aim to synthesize a MOF with hexagon 3D topology has been fulfilled.

It can be concluded that for all samples, there is a reaction that has occurred since the 16-17° peak in the PXRD data measurements, the strongest peak for all crystalline forms of the hexagon linker used, is not visible in any samples except for the VE-Zn3 sample. This means there has been a reaction between the metal salts and the organic linker H_6cpb.

This was also supported by TGA, IR and luminescence measurements.

For the specific lanthanoid samples made in the thesis, gadolinium and terbium, there is a big similarity between the samples, and the PXRD diffractogram more or less identical. This could indicate that they are iso-structural, as it is a reoccurring theme in this thesis, and the thesis written parallel to this thesis by Axel Jonsson.[insert reference!]

After reviewing structures in the CCDC database and swapping the found metal ions with gadolinium and terbium ions there were similarities between the thus simulated diffractogram of the known MOF CTH-9 [Co_4(cpb)(acetato)$_2$(dmf)$_4$] and the Gd-cpb and Tb-cpb PXRD data.

The use of a SAXS machine instead of a PXRD machine was tried in this thesis, and showed that the SAXS machine has a higher chance of finding peaks at low angles, as it is performed in vacuum which can remove a lot of disturbance. The first few samples that were tried in a regular PXRD did not show any crystallinity. The samples instead showed only one broad peak with much background noise. However, as the sample was analyzed by SAXS more similar spectra to literature appeared. SAXS diffractometer analysis needed less amount of sample compared to the PXRD available during the thesis.

In the far future when MOFs structures are confirmed, and their properties are fully analyzed, a way of mass-producing the MOF and especially the linker is the next step to commercially synthesize MOFs to improve the quality of human lives.

Bibliography

[1] Ishanie Perera, Champika Hettiarachchi, and Udayana Ranatunga. "Metal–Organic Frameworks in Dye-Sensitized Solar Cells". In: Jan. 2019, pp. 175–219. ISBN: 978-981-13-3301-9. DOI: 10.1007/978-981-13-3302-6{_}7.

[2] Stuart Batten et al. "Terminology of metal–organic frameworks and coordination polymers (IUPAC Recommendations 2013)*". In: *Pure and Applied Chemistry* 85 (Aug. 2013), pp. 1715–1724. DOI: 10.1351/PAC-REC-12-11-20.

[3] Omar M Yaghi. "Reticular Chemistry in All Dimensions". In: *ACS Central Science* 5.8 (Aug. 2019), pp. 1295–1300. ISSN: 2374-7943. DOI: 10.1021/acscentsci.9b00750. URL: https://doi.org/10.1021/acscentsci.9b00750.

[4] Kyle E Cordova and Omar M Yaghi. "The 'folklore' and reality of reticular chemistry". In: *Materials Chemistry Frontiers* 1.7 (2017), pp. 1304–1309. DOI: 10.1039/C7QM00144D. URL: http://dx.doi.org/10.1039/C7QM00144D.

[5] Weidong Fan et al. "Fine-Tuning the Pore Environment of the Microporous Cu-MOF for High Propylene Storage and Efficient Separation of Light Hydrocarbons". In: *ACS Central Science* 5.7 (July 2019), pp. 1261–1268. ISSN: 2374-7943. DOI: 10.1021/acscentsci.9b00423. URL: https://doi.org/10.1021/acscentsci.9b00423.

[6] Karen Leus et al. "A coordinative saturated vanadium containing metal organic framework that shows a remarkable catalytic activity". In: *Scientific Bases for the Preparation of Heterogeneous Catalysts*. Ed. by E M Gaigneaux et al. Vol. 175. Elsevier, 2010, pp. 329–332. ISBN: 0167-2991. DOI: https://doi.org/10.1016/S0167-2991(10)75053-9. URL: http://www.sciencedirect.com/science/article/pii/S0167299110750539.

[7] Ram Singh and Geetanjali. "25 - Metal organic frameworks for drug delivery". In: *Woodhead Publishing Series in Biomaterials*. Ed. by Inamuddin, Abdullah M Asiri, and Ali B T - Applications of Nanocomposite Materials in Drug Delivery Mohammad. Woodhead Publishing, 2018, pp. 605–617. ISBN: 978-0-12-813741-3. DOI: https://doi.org/10.1016/B978-0-12-813741-3.00026-1. URL: http://www.sciencedirect.com/science/article/pii/B9780128137413000261.

[8] Mohamed Eddaoudi et al. "Modular Chemistry: Secondary Building Units as a Basis for the Design of Highly Porous and Robust MetalOrganic Carboxylate Frameworks". In: *Accounts of Chemical Research* 34.4 (Apr. 2001), pp. 319–330. ISSN: 0001-4842. DOI: 10.1021/ar000034b. URL: https://doi.org/10.1021/ar000034b.

[9] Zheng-Bo Han et al. "Mn(II)-Based Porous Metal–Organic Framework Showing Metamagnetic Properties and High Hydrogen Adsorption at Low Pressure". In: *Inorganic Chemistry* 51.1 (Jan. 2012), pp. 674–679. ISSN: 0020-1669. DOI: 10.1021/ic2021929. URL: https://doi.org/10.1021/ic2021929.

[10] Mark D Allendorf, Raghavender Medishetty, and Roland A Fischer. "Guest molecules as a design element for metal–organic frameworks". In: *MRS Bulletin* 41.11 (2016), pp. 865–869. ISSN: 0883-7694. DOI: DOI:10.1557/mrs.2016.244. URL: https://www.cambridge.org/core/article/guest-molecules-as-a-design-element-for-metalorganic-frameworks/AFFF5E58A0413A2ED53A1190F578975E.

[11] Myunghyun Paik Suh et al. "Hydrogen Storage in Metal–Organic Frameworks". In: *Chemical Reviews* 112.2 (Feb. 2012), pp. 782–835. ISSN: 0009-2665. DOI: 10.1021/cr200274s. URL: https://doi.org/10.1021/cr200274s.

[12] Lauren E Kreno et al. "Metal–Organic Framework Materials as Chemical Sensors". In: *Chemical Reviews* 112.2 (Feb. 2012), pp. 1105–1125. ISSN: 0009-2665. DOI: 10.1021/cr200324t. URL: https://doi.org/10.1021/cr200324t.

[13] Jiewei Liu et al. "Applications of metal–organic frameworks in heterogeneous supramolecular catalysis". In: *Chemical Society Reviews* 43.16 (2014), pp. 6011–6061. ISSN: 0306-0012. DOI: 10.1039/C4CS00094C. URL: http://dx.doi.org/10.1039/C4CS00094C.

[14] Jian-Rong Li, Ryan J Kuppler, and Hong-Cai Zhou. "Selective gas adsorption and separation in metal–organic frameworks". In: *Chemical Society Reviews* 38.5 (2009), pp. 1477–1504. ISSN: 0306-0012. DOI: 10.1039/B802426J. URL: http://dx.doi.org/10.1039/B802426J.

[15] Yan Bai et al. "Zr-based metal-organic frameworks: Design, synthesis, structure, and applications". In: *Chemical Society reviews* 45 (Feb. 2016). DOI: 10.1039/c5cs00837a.

[16] Nicholas C Burtch, Himanshu Jasuja, and Krista S Walton. "Water Stability and Adsorption in Metal–Organic Frameworks". In: *Chemical Reviews* 114.20 (Oct. 2014), pp. 10575–10612. ISSN: 0009-2665. DOI: 10.1021/cr5002589. URL: https://doi.org/10.1021/cr5002589.

[17] John J Low et al. "Virtual High Throughput Screening Confirmed Experimentally: Porous Coordination Polymer Hydration". In: *Journal of the American Chemical Society* 131.43 (Nov. 2009), pp. 15834–15842. ISSN: 0002-7863. DOI: 10.1021/ja9061344. URL: https://doi.org/10.1021/ja9061344.

[18] Thomas Devic and Christian Serre. "High valence 3p and transition metal based MOFs". In: *Chemical Society Reviews* 43.16 (2014), pp. 6097–6115. ISSN: 0306-0012. DOI: 10.1039/C4CS00081A. URL: http://dx.doi.org/10.1039/C4CS00081A.

[19] Ping Lu et al. "What can pKa and NBO charges of the ligands tell us about the water and thermal stability of metal organic frameworks?" In: *Journal of Materials Chemistry A* 2.38 (2014), pp. 16250–16267. ISSN: 2050-7488. DOI: 10.1039/C4TA03154G. URL: http://dx.doi.org/10.1039/C4TA03154G.

[20] Jasmina Hafizovic Cavka et al. "A New Zirconium Inorganic Building Brick Forming Metal Organic Frameworks with Exceptional Stability". In: *Journal of the American Chemical Society* 130.42 (Oct. 2008), pp. 13850–13851. ISSN: 0002-7863. DOI: 10.1021/ja8057953. URL: https://doi.org/10.1021/ja8057953.

[21] Markus J Kalmutzki, Nikita Hanikel, and Omar M Yaghi. "Secondary building units as the turning point in the development of the reticular chemistry of MOFs". In: *Science Advances* 4.10 (Oct. 2018), eaat9180. DOI: 10.1126/sciadv.aat9180. URL: http://advances.sciencemag.org/content/4/10/eaat9180.abstract.

[22] Francoise M Amombo Noa et al. "Metal–Organic Frameworks with Hexakis(4-carboxyphenyl)benzene: Extensions to Reticular Chemistry and Introducing Foldable Nets". In: *Journal of the American Chemical Society* (Apr. 2020). ISSN: 0002-7863. DOI: 10.1021/jacs.0c02984. URL: https://doi.org/10.1021/jacs.0c02984.

[23] Phuong T K Nguyen et al. "Synthesis and Selective CO2 Capture Properties of a Series of Hexatopic Linker-Based Metal–Organic Frameworks". In: *Inorganic Chemistry* 54.20 (Oct. 2015), pp. 10065–10072. ISSN: 0020-1669. DOI: 10.1021/acs.inorgchem.5b01900. URL: https://doi.org/10.1021/acs.inorgchem.5b01900.

[24] Emil Kowalewski et al. "Turbostratic carbon supported palladium as an efficient catalyst for reductive purification of water from trichloroethylene". In: *AIMS Materials Science* 4.6 (2017), pp. 1276–1288. ISSN: 23720468. DOI: 10.3934/matersci.2017.6.1276. URL: http://www.aimspress.com/article/10.3934/matersci.2017.6.1276.

[25] Patrícia Silva et al. "Multifunctional metal–organic frameworks: from academia to industrial applications". In: *Chemical Society Reviews* 44.19 (2015), pp. 6774–6803. ISSN: 0306-0012. DOI: 10.1039/C5CS00307E. URL: http://dx.doi.org/10.1039/C5CS00307E.

[26] Lian Chen et al. "Metal–Organic Frameworks Based on Lanthanide Clusters BT - Lanthanide Metal-Organic Frameworks". In: ed. by Peng Cheng. Berlin, Heidelberg: Springer Berlin Heidelberg, 2015, pp. 145–183. ISBN: 978-3-662-45773-3. DOI: 10.1007/430{_}2014{_}161. URL: https://doi.org/10.1007/430_2014_161.

[27] Xiao-Yu Xu and Bing Yan. "Nanoscale LnMOF-functionalized nonwoven fibers protected by a polydimethylsiloxane coating layer as a highly sensitive ratiometric oxygen sensor". In: *Journal of Materials Chemistry C* 4.36 (2016), pp. 8514–8521. ISSN: 2050-7526. DOI: 10.1039/C6TC02569B. URL: http://dx.doi.org/10.1039/C6TC02569B.

[28] R D Shannon. "Revised effective ionic radii and systematic studies of interatomic distances in halides and chalcogenides". In: *Acta Crystallographica Section A* 32.5 (Sept. 1976), pp. 751–767. DOI: 10.1107/S0567739476001551. URL: https://doi.org/10.1107/S0567739476001551.

[29] Sarah L Griffin and Neil R Champness. "A periodic table of metal-organic frameworks". In: *Coordination Chemistry Reviews* 414 (2020), p. 213295. ISSN: 0010-8545. DOI: https://doi.org/10.1016/j.ccr.2020.213295. URL: http://www.sciencedirect.com/science/article/pii/S0010854519307799.

[30] Jinzeng Wang et al. "A terbium metal–organic framework with stable luminescent emission in a wide pH range that acts as a quantitative detection material for nitroaromatics". In: *RSC Advances* 5.60 (2015), pp. 48574–48579. DOI: 10.1039/C5RA06308F. URL: http://dx.doi.org/10.1039/C5RA06308F.

[31] Kathryn M. L. Taylor, Athena Jin, and Wenbin Lin. "Surfactant-Assisted Synthesis of Nanoscale Gadolinium Metal–Organic Frameworks for Potential Multimodal Imaging". In: *Angewandte Chemie International Edition* 47.40 (Sept. 2008), pp. 7722–7725. ISSN: 1433-7851. DOI: 10.1002/anie.200802911. URL: https://doi.org/10.1002/anie.200802911.

[32] A Dean Sherry, Peter Caravan, and Robert E Lenkinski. "Primer on gadolinium chemistry". eng. In: *Journal of magnetic resonance imaging : JMRI* 30.6 (Dec. 2009), pp. 1240–1248. ISSN: 1522-2586. DOI: 10.1002/jmri.21966. URL: https://pubmed.ncbi.nlm.nih.gov/19938036%20https://www.ncbi.nlm.nih.gov/pmc/articles/PMC2853020/.

[33] Piwai Tshuma et al. "Cyclometalation of lanthanum(iii) based MOF for catalytic hydrogenation of carbon dioxide to formate". In: *RSC Advances* 10.6 (2020), pp. 3593–3605. DOI: 10.1039/C9RA09938G. URL: http://dx.doi.org/10.1039/C9RA09938G.

[34] Weiyi Ouyang et al. "Chapter 5 - Nanoparticles within functional frameworks and their applications in photo(electro)catalysis". In: *Micro and Nano Technologies*. Ed. by Julia Pérez Prieto and María González B T - Photoactive Inorganic Nanoparticles Béjar. Elsevier, 2019, pp. 109–138. ISBN: 978-0-12-814531-9. DOI: https://doi.org/10.1016/B978-0-12-814531-9.00005-1. URL: http://www.sciencedirect.com/science/article/pii/B9780128145319000051.

[35] Jianping Lai et al. "Solvothermal synthesis of metal nanocrystals and their applications". In: *Nano Today* 10.2 (2015), pp. 240–267. ISSN: 1748-0132. DOI: https://doi.org/10.1016/j.nantod.2015.03.001. URL: http://www.sciencedirect.com/science/article/pii/S1748013215000316.

[36] Deena R Modeshia and Richard I Walton. "Solvothermal synthesis of perovskites and pyrochlores: crystallisation of functional oxides under mild conditions". In: *Chemical Society Reviews* 39.11 (2010), pp. 4303–4325. ISSN: 0306-0012. DOI: 10.1039/B904702F. URL: http://dx.doi.org/10.1039/B904702F.

[37] Jian Li and Junliang Sun. "Application of X-ray Diffraction and Electron Crystallography for Solving Complex Structure Problems". In: *Accounts of Chemical Research* 50.11 (Nov. 2017), pp. 2737–2745. ISSN: 0001-4842. DOI: 10.1021/acs.accounts.7b00366. URL: https://doi.org/10.1021/acs.accounts.7b00366.

[38] Andrei A Bunaciu, Elena UdriŞTioiu, and Hassan Aboul-Enein. "X-Ray Diffraction: Instrumentation and Applications". In: *Critical reviews in analytical chemistry / CRC* 45 (Apr. 2015). DOI: 10.1080/10408347.2014.949616.

[39] Lesley E Smart and Elaine A Moore. *Solid state chemistry: an introduction*. CRC press, 2012. ISBN: 1439847908.

[40] Komang Suastika et al. "Characterization of Central Kalimantan's Amethysts by Using X-Ray Diffraction". In: *Journal of Physics: Conference Series* 846 (May 2017), p. 12024. DOI: 10.1088/1742-6596/846/1/012024.

[41] Zhehao Huang et al. "Can 3D Electron Diffraction Provide Accurate Atomic Structures of Metal-Organic Frameworks?" In: (2020). DOI: 10.26434/chemrxiv.11688270.v1. URL: https://chemrxiv.org/articles/Can_3D_Electron_Diffraction_Provide_Accurate_Atomic_Structures_of_Metal-Organic_Frameworks_/11688270.

[42] S T Misture and R L Snyder. "X-ray Diffraction". In: ed. by K H Jürgen Buschow et al. Oxford: Elsevier, 2001, pp. 9799–9808. ISBN: 978-0-08-043152-9. DOI: https://doi.org/10.1016/B0-08-043152-6/01778-2. URL: http://www.sciencedirect.com/science/article/pii/B0080431526017782.

[43] J M Cowley. "Crystal structure determination by electron diffraction". In: *Progress in Materials Science* 13 (1968), pp. 267–321. ISSN: 0079-6425. DOI: https://doi.org/10.1016/0079-6425(68)90023-6. URL: http://www.sciencedirect.com/science/article/pii/0079642568900236.

[44] Tobias Starborg et al. "Experimental steering of electron microscopy studies using prior X-ray computed tomography". In: *Ultramicroscopy* 201 (2019), pp. 58–67. ISSN: 0304-3991. DOI: https://doi.org/10.1016/j.ultramic.2019.03.002. URL: http://www.sciencedirect.com/science/article/pii/S0304399118304443.

[45] "Chapter 3 - Methods for Assessing Surface Cleanliness". In: ed. by Rajiv Kohli, K L B T - Developments in Surface Contamination Mittal Volume 12, and Cleaning. Elsevier, 2019, pp. 23–105. ISBN: 978-0-12-816081-7. DOI: https://doi.org/10.1016/B978-0-12-816081-7.00003-6. URL: http://www.sciencedirect.com/science/article/pii/B9780128160817000036.

[46] Rajiv Kohli. "Chapter 3 - Methods for Monitoring and Measuring Cleanliness of Surfaces". In: ed. by Rajiv Kohli, K L B T - Developments in Surface Contamination Mittal, and Cleaning. Oxford: William Andrew Publishing, 2012, pp. 107–178. ISBN: 978-1-4377-7883-0. DOI: https://doi.org/10.1016/B978-1-4377-7883-0.00003-1. URL: http://www.sciencedirect.com/science/article/pii/B9781437778830000031.

[47] W M GROENEWOUD. "CHAPTER 2 - THERMOGRAVIMETRY". In: ed. by W M B T - Characterisation of Polymers by Thermal Analysis GROENEWOUD. Amsterdam: Elsevier Science B.V., 2001, pp. 61–76. ISBN: 978-0-444-50604-7. DOI: https://doi.org/10.1016/B978-044450604-7/50003-0. URL: http://www.sciencedirect.com/science/article/pii/B9780444506047500030.

[48] Sergey Ivanov. "Chapter 7 - Multiferroic complex metal oxides: Main features of preparation, structure, and properties". In: *Advanced Functional Materials*. Ed. by Tara Prasad Das et al. Vol. 2. Elsevier, 2012, pp. 163–238. ISBN: 1875-4023. DOI: https://doi.org/10.1016/B978-0-44-453681-5.00007-8. URL: http://www.sciencedirect.com/science/article/pii/B9780444536815000078.

[49] S Bandyopadhyay-Ghosh, S B Ghosh, and M Sain. "19 - The use of biobased nanofibres in composites". In: ed. by Omar Faruk and Mohini B T - Biofiber Reinforcements in Composite Materials Sain. Woodhead Publishing, 2015, pp. 571–647. ISBN: 978-1-78242-122-1. DOI: https://doi.org/10.1533/9781782421276.5.571. URL: http://www.sciencedirect.com/science/article/pii/B9781782421221500198.

[50] James Gomes et al. "Chapter 25 - Monitoring and Control of Bioethanol Production From Lignocellulosic Biomass". In: ed. by Thallada Bhaskar et al. Elsevier, 2018, pp. 727–749. ISBN: 978-0-444-63992-9. DOI: https://doi.org/10.1016/B978-0-444-63992-9.00025-2. URL: http://www.sciencedirect.com/science/article/pii/B9780444639929000252.

[51] Gadipelli Srinivas and Z Xiao Guo. "Postsynthesis Annealing of MOF-5 Remarkably Enhances the Framework Structural Stability and CO 2 Uptake". In: *Chemistry of Materials* 26 (Oct. 2014). DOI: 10.1021/cm502399q.

[52] H W B T - Reference Module in Materials Science Siesler and Materials Engineering. "Vibrational Spectroscopy". In: Elsevier, 2016. ISBN: 978-0-12-803581-8. DOI: https://doi.org/10.1016/B978-0-12-803581-8.01318-7. URL: http://www.sciencedirect.com/science/article/pii/B9780128035818013187.

[53] Yunchen Wang et al. "Elucidation of the elusive structure and formula of the active pharmaceutical ingredient bismuth subgallate by continuous rotation electron diffraction". In: *Chemical Communications* 53.52 (2017), pp. 7018–7021. ISSN: 1359-7345. DOI: 10.1039/C7CC03180G. URL: http://dx.doi.org/10.1039/C7CC03180G.

[54] Clare F Macrae et al. "{\it Mercury 4.0}: from visualization to analysis, design and prediction". In: *Journal of Applied Crystallography* 53.1 (Feb. 2020), pp. 226–235. DOI: 10.1107/S1600576719014092. URL: https://doi.org/10.1107/S1600576719014092.

[55] Quan Li, Tao Li, and Jinguang Wu. "Luminescence of Europium(III) and Terbium(III) Complexes Incorporated in Poly(Vinyl Pyrrolidone) Matrix". In: *The Journal of Physical Chemistry B* 105.49 (Dec. 2001), pp. 12293–12296. ISSN: 1520-6106. DOI: 10.1021/jp012922+. URL: https://doi.org/10.1021/jp012922+.

[56] Yi Wang et al. "Hydrogen photochromism in V2O5 layers prepared by sol–gel technology with the use of dimethylformamide as a hydrogen donor". In: *Journal of Sol-Gel Science and Technology* 86 (Mar. 2018). DOI: 10.1007/s10971-018-4614-1.

[57] Axel Jonsson. "Synthesis and development of hexagon based metal-organic frameworks". PhD thesis. Chalmers University of Technology, 2020, p. 40.

Appendix 1

A1 Microscope pictures

Here the documented pictures of the different samples that were synthesized are presented. Only somewhat successful synthesized samples were documented as burnt or non-crystalline samples where discarded.

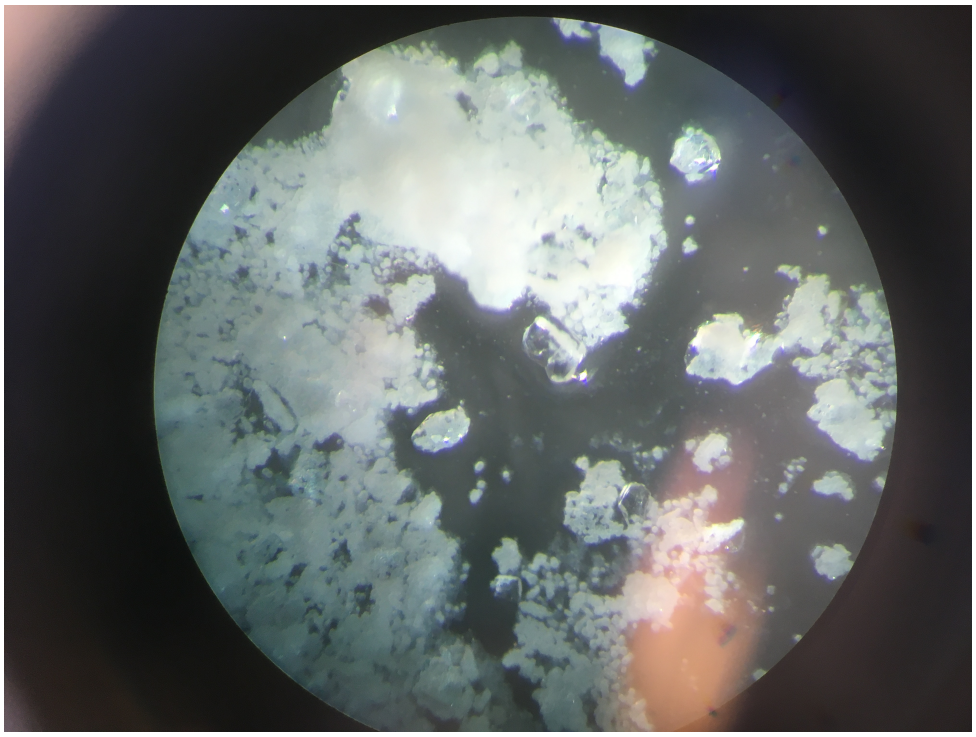

Figure A1: Picture of the VE-Tb1 sample after heating in oven

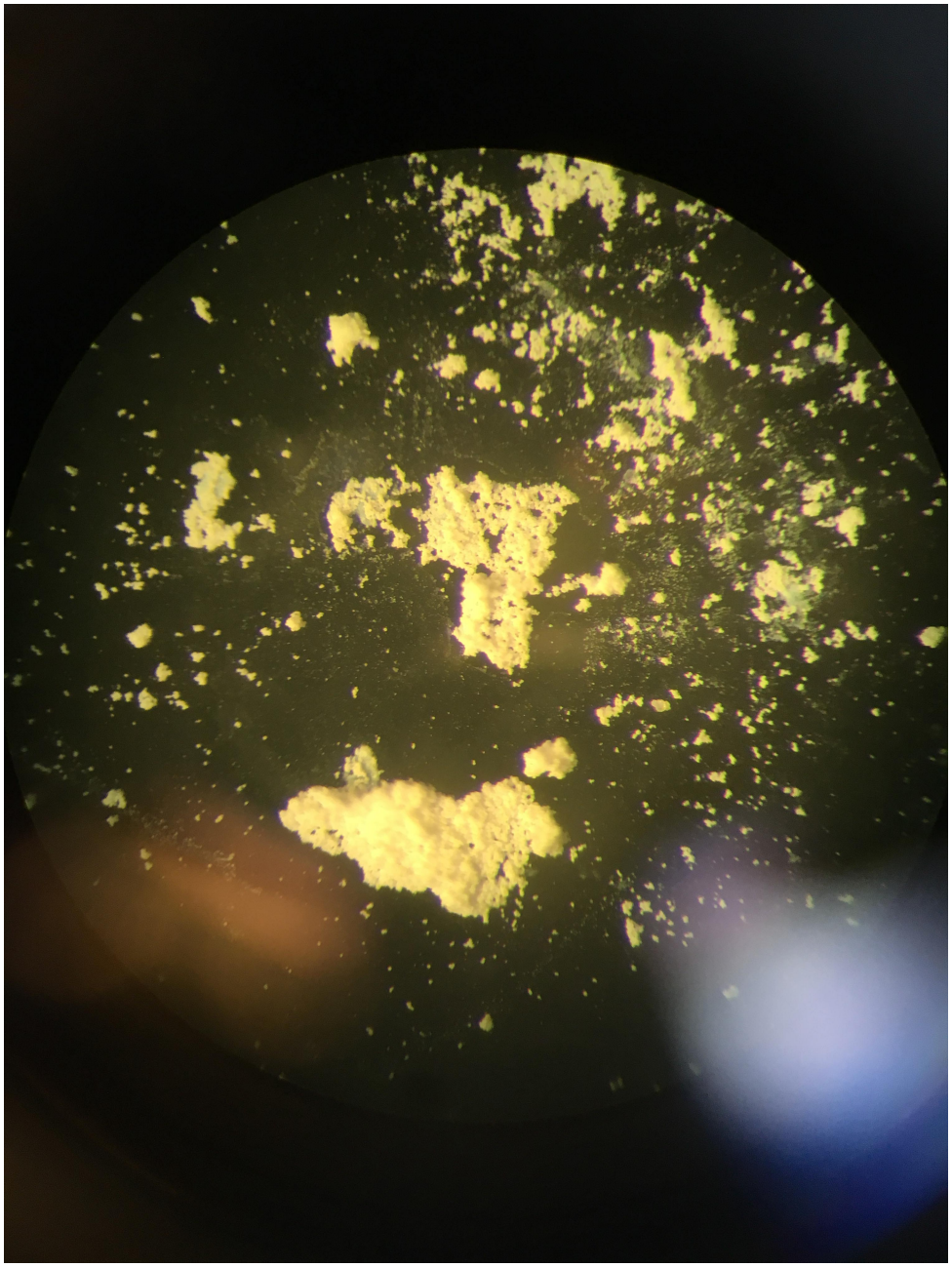

Figure A2: Picture of the VE-Tb3 sample after heating in oven

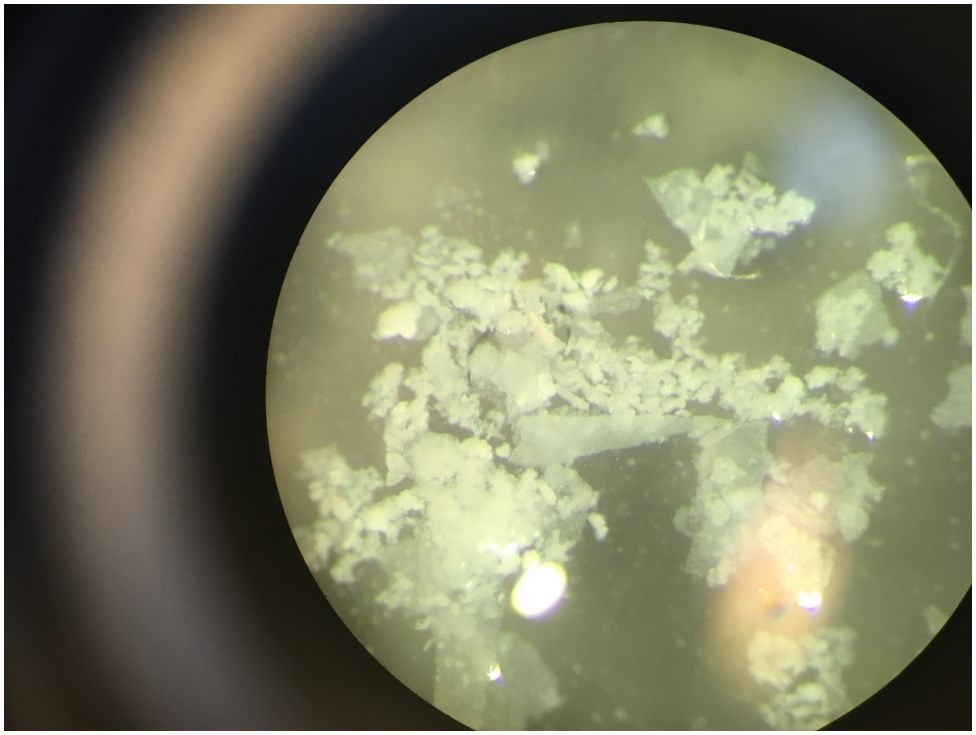

Figure A3: Picture of the VE-Al1 sample after heating in oven

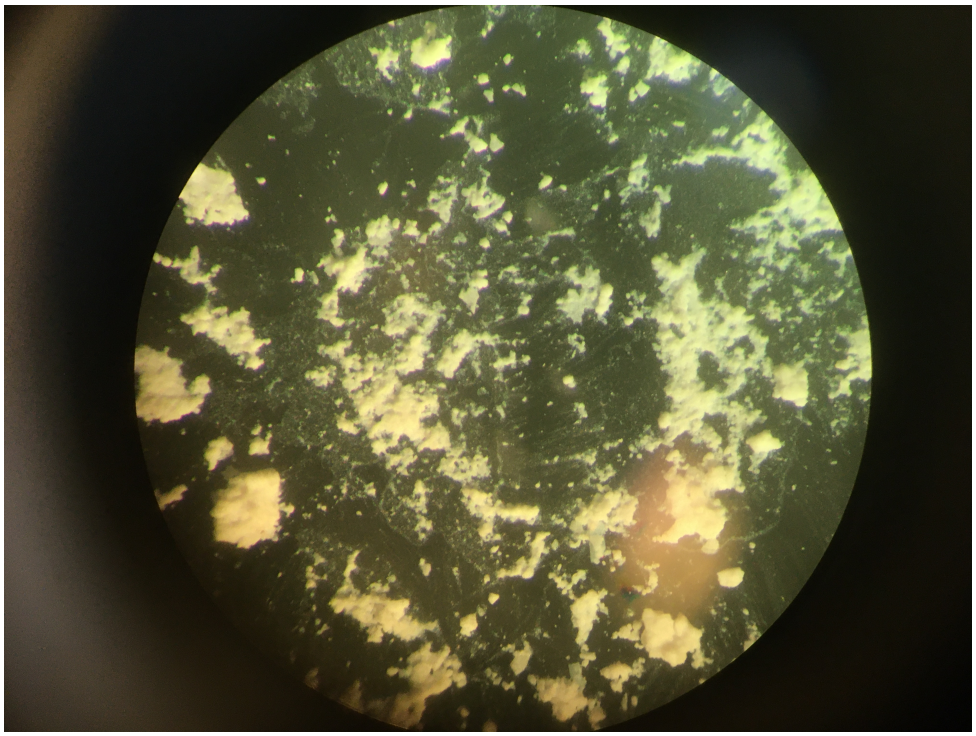

Figure A4: Picture of the VE-Al3 sample after heating in oven

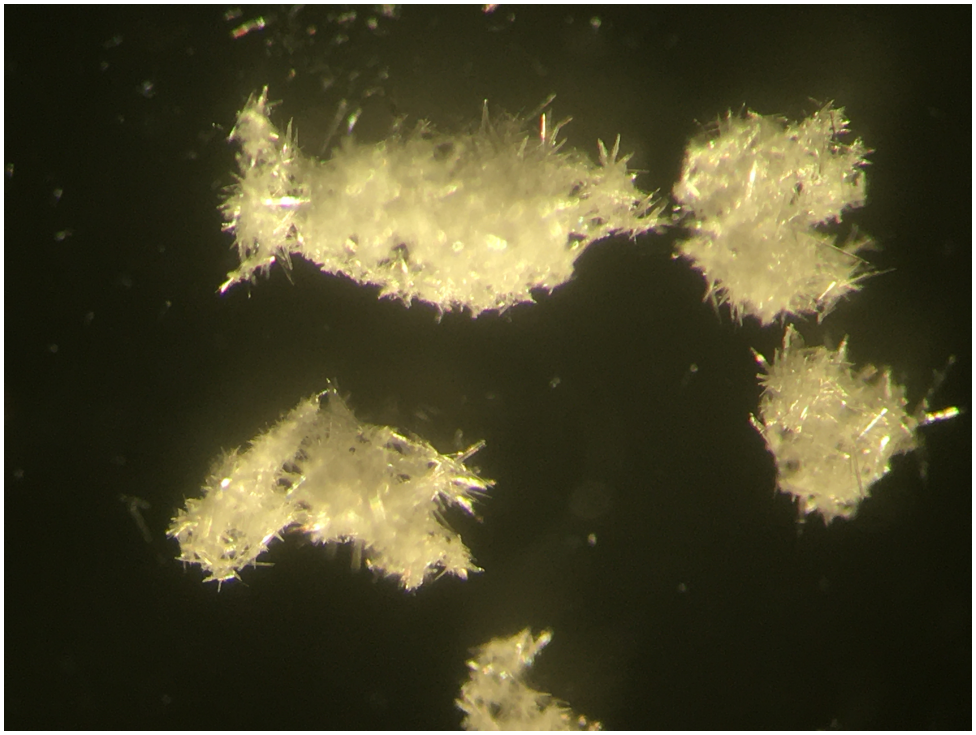

Figure A5: Picture of the VE-Zn1 sample after heating in oven

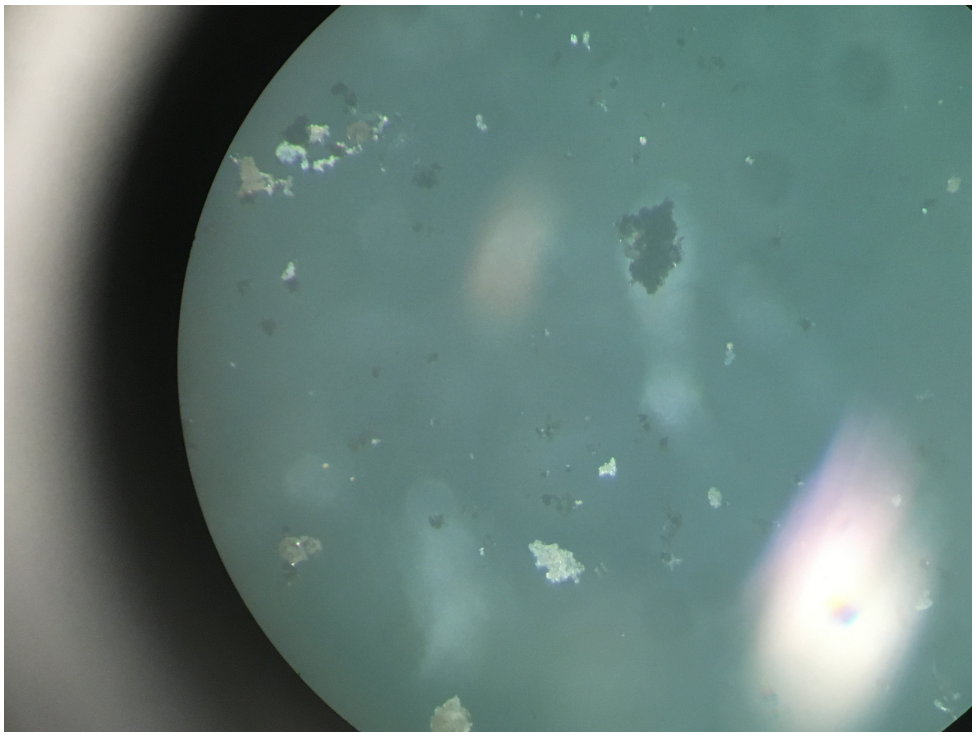

Figure A6: Picture of the VE-Zn+ppb sample after heating in oven

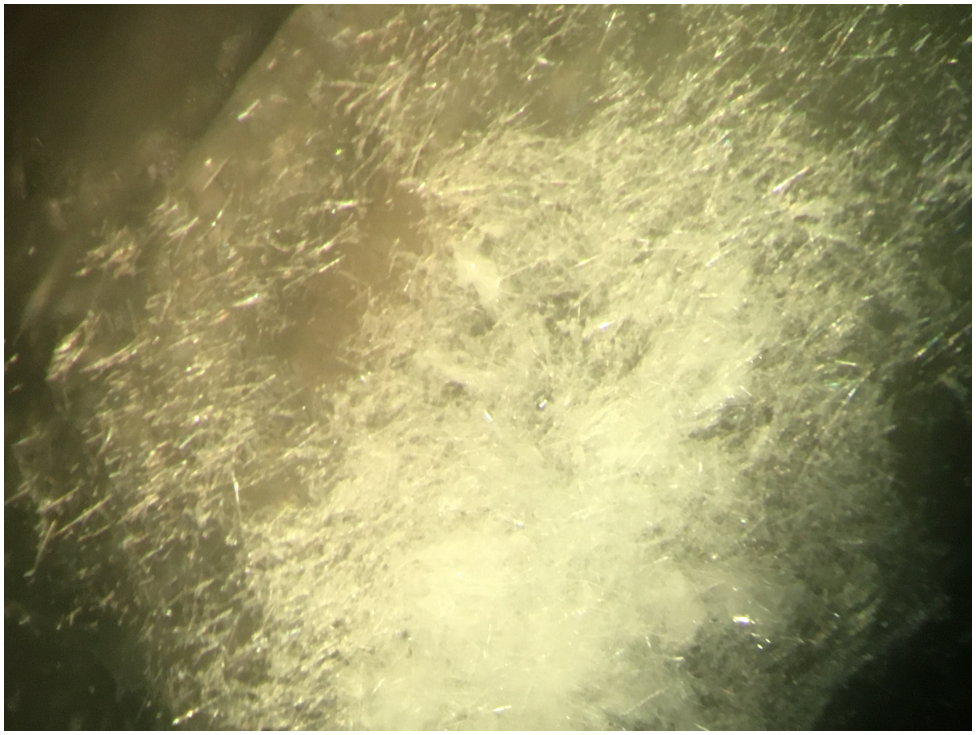

Figure A7: Picture of the VE-Mn1 sample after heating in oven

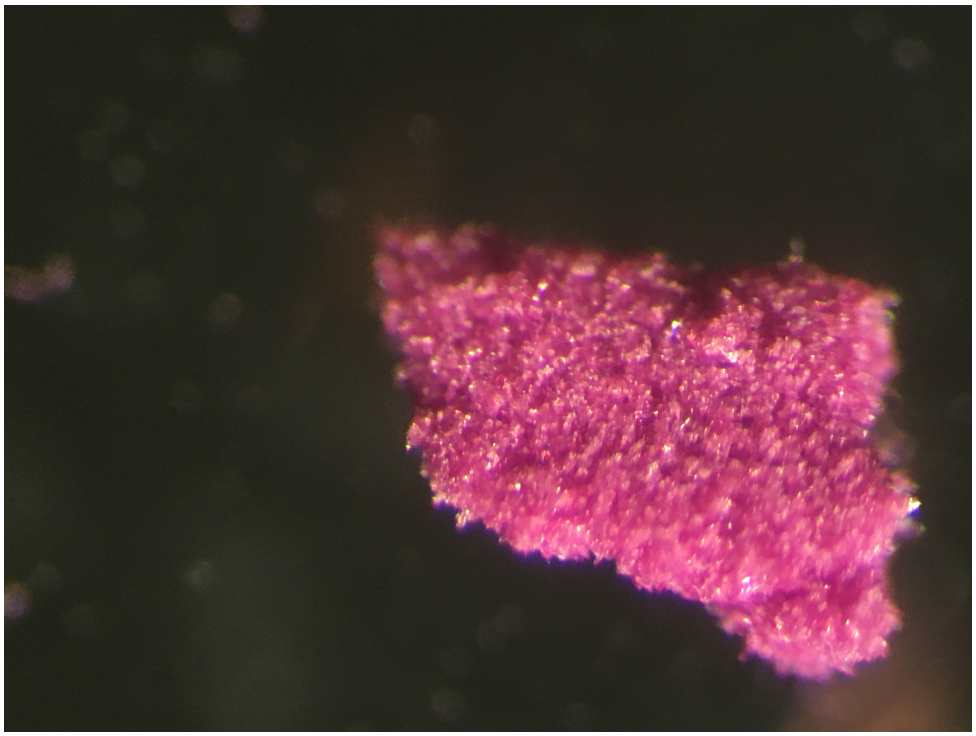

Figure A8: Picture of the VE-Co1 sample after heating in oven

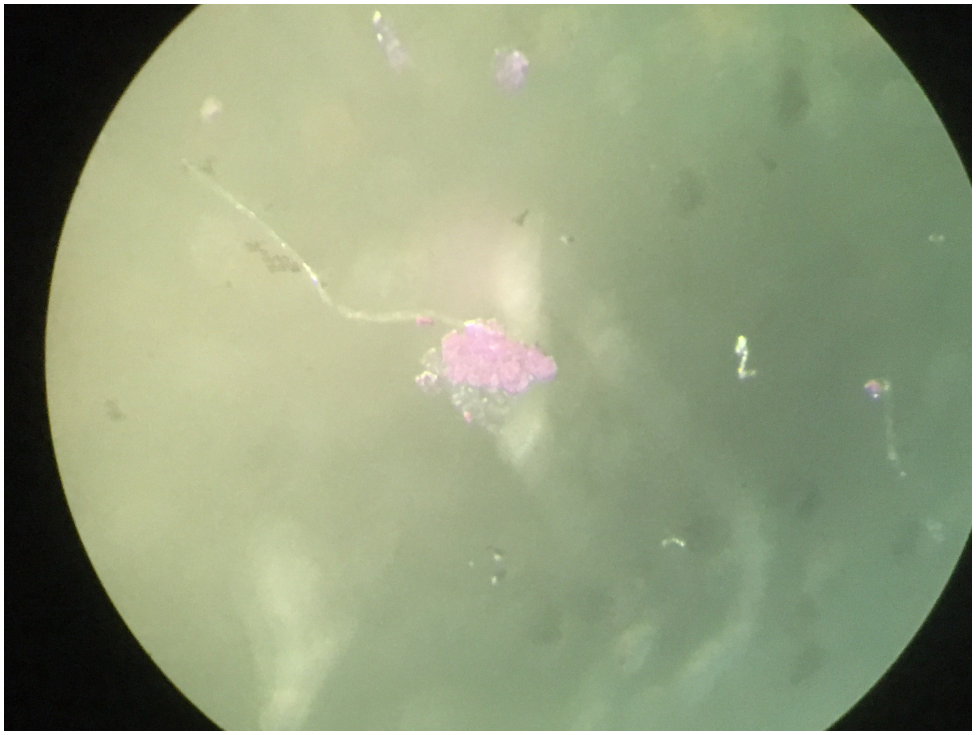

Figure A9: Picture of the VE-Co+ppb sample after heating in oven

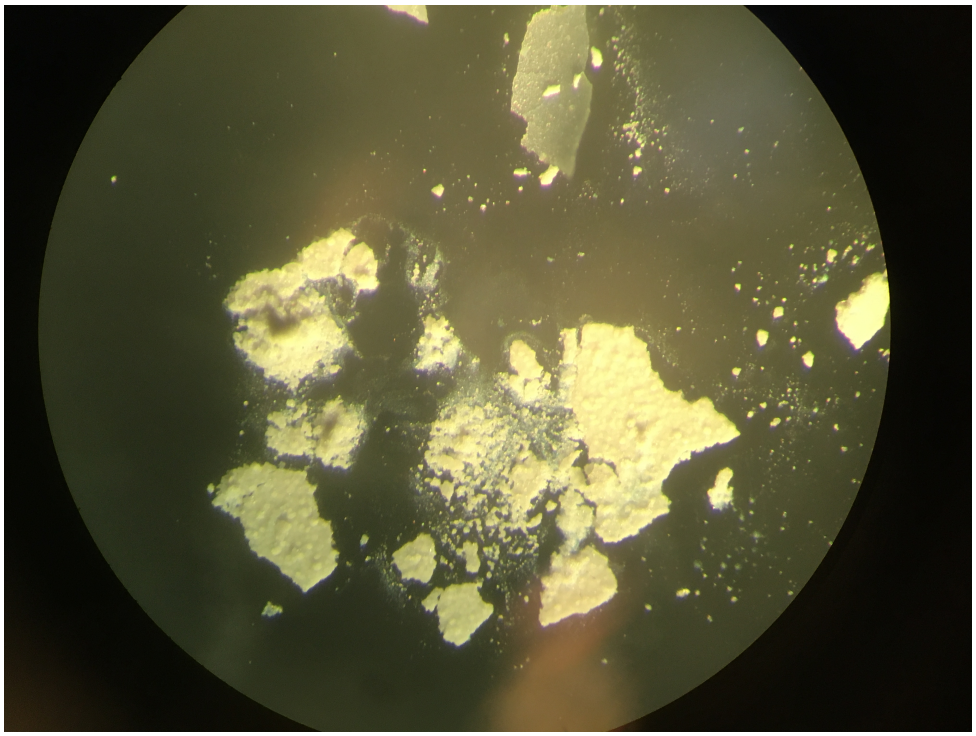

Figure A10: Picture of the VE-V2 sample after heating in oven

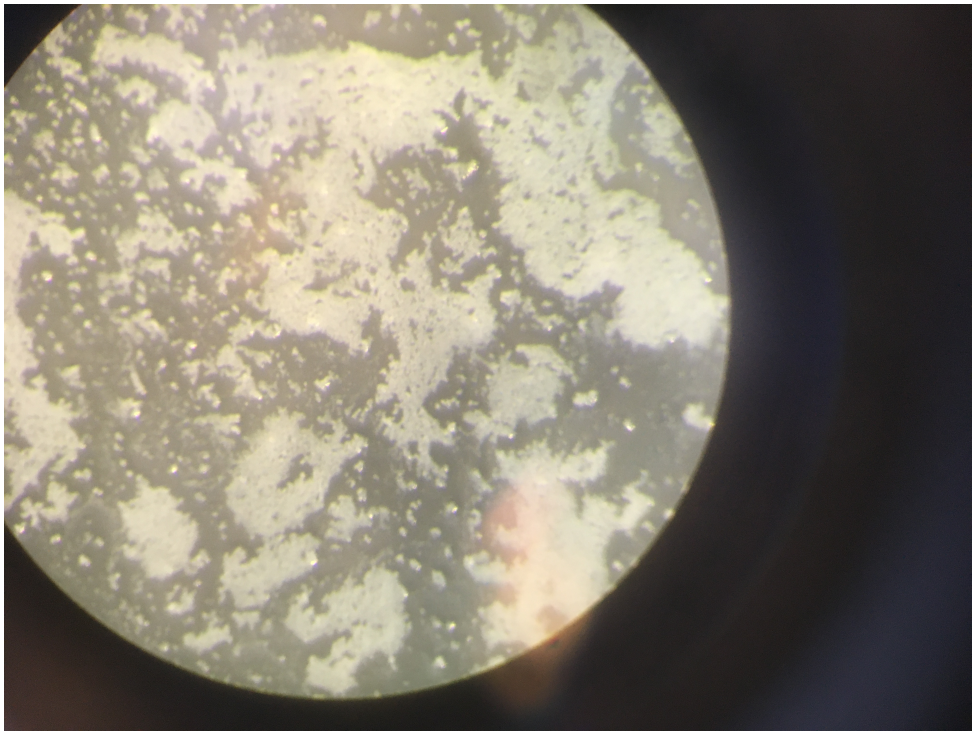

Figure A11: Picture of the VE-Zr3 sample after heating in oven

A2 SAXS diffractometer

The machinery used was a SAXSLAB Mat:Nordic instrument equipped with a micro-focus Cu X-ray source (lambda=1.54Å) and a Dectris Pilatus 300K R ($3° \leq 2\theta \leq 30°$-in line with the beam) and 100K R ($28° \leq 2\theta \leq 85°$ - mounted on a motorized goniometer) detectors. Air scattering was removed by reducing the pressure to 0.2 mbar in the general path of the beam. All sample positions were calibrated 20 minutes on both detectors per sample before analyzation would begin. In the case of this thesis the detector was first placed at 39°and next at 57°this resulted in a angular range of 28°-50°(2θ) and 46°-68°where the overlap was averaged in the data merging.

A3 Heating programs

Here information about the specific heating programs used in the Memmert oven is provided. If no heat program was used, information of how long it was placed in an oven that is around 120°C could be found in table **??** and **??** for MOF recipes 1 and 2 respectively.

Heating program 1*

Heating program 1* was started by a temperature increase gradient from 20°C to 120°C over 2 hours. The sample was then heated for 96 hours (4 days) at 120°C to then be cooled slowly for 70 hours from 120°C to 20°C.

Heating program 2*

Heating program 2* was started by a temperature increase gradient from 20°C to 150°C over 2 hours. The sample was then heated for 168 hours at 150°C and was then cooled slowly for 20 hours from 150°C to 20°C.

Heating program 3*

Heating program 3* was started by a temperature increase gradient from 20°C to 150°C over 2 hours. The sample was then heated for 336 hours at 150°C and was then cooled slowly for 20 hours from 150°C to 20°C.